CONTRIBUTIONS TO ZOOLOGY (2022) 1–34

BRILL

CTOZ
brill.com/ctoz

Growth and limb bone histology of aetosaurs and phytosaurs from the Late Triassic Krasiejów locality (SW Poland) reveals strong environmental influence on growth pattern

Elżbieta M. Teschner | ORCID: 0000-0001-5961-489X
Institute of Biology, Opole University, Oleska 22, 45-052 Opole, Poland
Department of Paleontology, Institute of Geosciences, Rheinische Friedrichs-Wilhelm-Universitat Bonn, Nussallee 8, 53115 Bonn, Germany
eteschner@uni.opole.pl

Dorota Konietzko-Meier
Department of Paleontology, Institute of Geosciences, Rheinische Friedrichs-Wilhelm-Universität Bonn, Nussallee 8, 53115 Bonn, Germany

Nicole Klein
Department of Paleontology, Institute of Geosciences, Rheinische Friedrichs-Wilhelm-Universität Bonn, Nussallee 8, 53115 Bonn, Germany
Paleontological Institute and Museum, University of Zurich, Karl-Schmid-Strasse 4, 8006 Zurich, Switzerland

RECEIVED: 8 DECEMBER 2021 | REVISED AND ACCEPTED: 3 APRIL 2022
EDITOR: A.A.E. VAN DER GEER

Abstract

The growth pattern of the Polish phytosaur *Parasuchus* cf. *arenaceus* and the aetosaur *Stagonolepis olenkae* (both Krasiejów; Norian) was studied. Results were compared to published data of other members of these two groups and to a new sample of the German (Heslach; Norian) phytosaur *Nicrosaurus* sp. All three herein studied taxa display lamellar-zonal bone consisting predominately of parallel-fibred tissue and on average a low to moderate vascular density. Towards the outer cortex the thickness of annuli increases in most samples and becomes distinctly wider than the zones. Therefore, most of the appositional growth in adults was achieved during phases of prolonged slow growth. All bones show a diffuse growth pattern, without well demarcated zones and annuli. Distinct lines of arrested growth (LAG) are not identified in the Krasiejów sample, only the *Nicrosaurus* femur shows one distinct LAG as do other taxa outside Krasiejów. Instead, the Krasiejów taxa display multiple rest lines and sub-cycles.

Thus, identification and count of annual growth cycles remains difficult, the finally counted annual growth cycles range (two to six) is quite large despite the low size range of the samples. A correlation between age and bone length is not identified, indicating developmental plasticity. Although both are archosaurs, *Stagonolepis* and *Parasuchus* are phylogenetically not closely related, however, they show a very similar growth pattern, despite different life styles (terrestrial vs. semi-aquatic). Based on the new data, and previously histological studies from Krasiejów, the local environmental conditions were special and had a strong influence on the growth pattern.

Keywords

absence of lines of arrested growth (LAGs) – environmental influence – growth marks – growth record – microanatomy – rest lines

Introduction

Palaeohistological analyses performed on bones are a valuable source of biological information e.g., growth rate and age of extinct animals, as well as indirectly local environmental conditions (de Buffrénil et al., 2021). As an answer to adaptation in various local life conditions, vertebrates lay down cyclical (in most cases annual) growth marks (Francillon-Vieillot et al., 1990). They appear to reflect a seasonal change of the conditions, deposited as layers of fast-growing tissue (zones), created most probably during a favourable season, and slow-growing or even temporary cessed growth (annuli and/or line of arrested growth [LAG]), connected with an unfavourable phase during life (Francillon-Vieillot et al., 1990). For endothermic vertebrates the cyclicity seems to be determined genetically as showed by e.g., Köhler et al. (2012) who studied the growth pattern of wild ruminants living across different climatic zones, from polar to tropical environments, but depositing the same tissue and growth marks. This demonstrates that the annual formation of LAGs for homeothermic endotherm animals, is controlled genetically (hormonally) rather than resulting from environmental stresses (Köhler et al., 2012). In poikilotherm animals the influence of external conditions in the growth record is due to physiological constrains better visible as in homeothermic animals (see de Buffrénil et al., 2021). However, how the growth pattern of the poikilothermic animals is influenced by the environment, is understudied. Analyses of different taxa originating from the same locality and time, might shed new light on this question.

The perspective of multi-taxic histological studies

The rarity of multi-taxic osteohistological studies in palaeontology is related to the lack of enough adequate material and/or the destructive nature of histological analyses. The Krasiejów locality (southwestern Poland) provides a unique window into the Late Triassic ecosystem (Dzik & Sulej, 2007) due to a remarkable quality and the quantity of the excavated bones. Jewuła et al. (2019) studied the genesis of various Late Triassic deposits in the Upper Silesia region and proposed a gilgai (i.e., ephemeral stream system) environment for the Krasiejów deposits attributed to sedimentological evidence for semi-dry, seasonal

climatic variation. The high number of skeletal elements preserved in Krasiejów presents a good opportunity to study the histology of taxa coexisting in one locality in the same horizon. The preserved tetrapod taxa include the remains of temnospondyl amphibians: *Metoposaurus krasiejowensis* (Sulej, 2007) and *Cyclotosaurus intermedius* Sulej & Majer, 2005, but also archosaurs: the aetosaur *Stagonolepis olenkae* Sulej, 2010, the phytosaur *Parasuchus* cf. *arenaceus* (Dzik, 2001; Dzik & Sulej, 2007), the 'rauisuchid' *Polonosuchus silesiacus* (Sulej, 2005), the dinosauriform *Silesaurus opolensis* Dzik, 2003, and the protorosaur *Ozimek volans* Dzik & Sulej, 2016. So far, the histology of the aquatic temnospondyl *M. krasiejowensis* from Krasiejów was studied in detail, based on almost all skeletal elements (Gądek, 2012; Gruntmejer et al., 2016, 2019, 2021; Konietzko-Meier et al., 2012, 2014, 2018; Konietzko-Meier & Klein, 2013; Konietzko-Meier & Sander, 2013; Teschner et al., 2018, 2020). The long bones of *M. krasiejowensis* show an alternating pattern of zones and annuli without LAGs, including prolonged phases of slow growth, multiple sub-cycles and rest lines. The documented growth record of *Metoposaurus* indicates a moderate, less seasonal climate at Krasiejów, after the comparison with the growth record to similarly aged (Norian) and phylogenetically related taxa from India and Morocco (Konietzko-Meier & Klein, 2013; Teschner et al., 2018). Femora, tibiae, a metatarsal, and ribs of the terrestrial dinosauriform *Silesaurus opolensis* were studied histologically (Fostowicz-Frelik & Sulej, 2010). They display a nearly uninterrupted fibro-lamellar bone (FLB) with only the outermost cortex becoming higher organized and less dense vascular, absence of LAGs, except for one tibia possessing one LAG. Fostowicz-Frelik & Sulej (2010) suggested that the lack of clear growth marks could be related with the hypothetical endothermy of that taxon, however, the sectioned material was insufficient to prove this due to a limited material sectioned.

The analysis of the two most common archosaurs in Krasiejów, an aetosaur and a phytosaur, originating from the same horizon, might contribute to answer the question, how distantly related, poikilotherm amniotes reacted to the same environmental conditions.

Taxonomy and depositional environment

Two major archosaur groups, Aetosauria (Marsh, 1884) and Phytosauria (Jäger, 1828), are a constant component of Late Triassic (Carnian to Rhaetian) faunal assemblage found on almost all continents (Buffetaut, 1993; Lucas, 1998; Desojo et al., 2013; Stocker & Butler, 2013; Barrett et al., 2020). The only exception is *Diandogosuchus* from the Middle Triassic of China (Li et al., 2012; Stocker et al., 2017), representing so far, the oldest and phylogenetically most basal phytosaur (Butler et al., 2019). Aetosauria are interpreted as being herbivorous to omnivorous in diet and occupying terrestrial habitats (Carroll, 1988; Small, 2002; Desojo & Vizcaino, 2009; Desojo et al., 2013). Phytosaurs are mostly found in lacustrine and fluviatile environments worldwide (Hungerbühler, 2000; Stocker & Butler, 2013) and their mode of life was reconstructed as semi-aquatic to aquatic (Hunt, 1989). There are also marine phytosaur representatives from Europe e.g., Austria and Italy (Buffetaut, 1993; Renesto & Paganoni, 1998; Gozzi & Renesto, 2003; Renesto, 2008; Butler et al., 2019) and China (Li et al., 2012).

The aetosaur material from Krasiejów is represented by multiple disarticulated skeletal elements for which a new species was erected within the genus *Stagonolepis*: *S. olenkae* Sulej, 2010. The validity of the discrimination of *S. olenkae* from the Scottish *S. robertsoni* was questioned by Antczak (2016), who suggested, based on the examination of

new material that both belong to the same species and differences are related to individual variation and possible sexual dimorphism. Recently, an aetosaurian pes from Krasiejów was described morphologically, without a definitive assignment to *S. olenkae*, moreover, the authors could not exclude a possible co-occurrence of two aetosaur species in Krasiejów (Górnicki et al., 2021). However, the exact taxonomical assignment of our sample is not within the scope of this study and likely irrelevant as both species seem to have similar niches.

The morphology and phylogenetic relationship of the phytosaurs from Krasiejów is understudied (Butler et al., 2014) when compared to other phytosaur specimens from Europe (Hungerbühler, 2000, 2002; Brusatte et al., 2013; Mateus et al., 2014, Butler et al., 2019). Dzik (2001) first proposed affinity of the Polish material to *'Paleorhinus'* sp. and later Dzik & Sulej (2007) proposed the affinity of the material to *'Paleorhinus'* cf. *arenaceus*. However, the taxon from Krasiejów was so far not included in any phylogenetic analysis. The species from Krasiejów is considered as a basal representative within Phytosauria due to the anterior position of the nares (Dzik, 2001; Dzik & Sulej, 2007). Other *'Paleorhinus'* specimens have been reported from Germany and USA (Lees, 1907; Hunt & Lucas, 1991; Butler et al., 2014) whereas *Parasuchus* was described from India (Chatterjee, 1978). However, according to Case 3165 of the International Code of Zoological Nomenclature, the genus *Parasuchus* took priority over *'Paleorhinus'* (Chatterjee, 2001; Kammerer et al., 2016; Jones & Butler, 2018) and both taxa now represent a single taxon. Again, the exact taxonomic affiliation of the phytosaur from Krasiejów is not relevant and beyond the scope of the current study.

The age of the Krasiejów deposits is still debated due to the lack of index fossils or palynological data (Szulc, 2005). Dzik et al. (2000) favours a Carnian age based on biostratigraphy and the correlation with dated beds known from southern Germany (Lehrberg Beds; Dzik et al., 2000) and a lacustrine origin of the deposits (Dzik et al., 2000; Dzik & Sulej, 2007, 2016). However, subsequent extensive sedimentological, lithostratigraphic and taphonomic studies supported a Norian age for the deposits (Szulc, 2005; Bodzioch & Kowal-Linka, 2012; Szulc & Racki, 2015; Szulc et al., 2015, 2017) and a fluviatile origin caused by an ephemeral stream system under semi-dry climatic conditions (Szulc, 2005). Bodzioch & Kowal-Linka (2012) reconstructed a more catastrophic origin of the bone bed caused by a short-lived but high-energy flood event resulting in hydraulically segregated bone breccia, accumulating the disarticulated skeletons in the vicinity of what is today the clay pit.

Heslach, is a Late Triassic (Norian) locality in southern Germany near Stuttgart. The phytosaur *Nicrosaurus kapffi* (von Meyer, 1861), was found in fluviatile deposits of the Stubensandstein Formation (Nitsch, 2006), and is phylogenetically considered to represent a more derived specimen when compared to the Polish taxon (Hungerbühler, 2002; Kimmig, 2013). Based on the femoral morphology of *Nicrosaurus*, a semi-aquatic or even a secondarily terrestrial mode of life has been proposed (Kimmig, 2013). No sedimentological studies are known for this locality, thus no inference about the climatic conditions during the Norian in Heslach can be made.

Histology research on aetosaurs and phytosaurs to date

Histologically, the best studied elements of aetosaurs and phytosaurs are their osteoderms (Parker et al., 2008; Cerda & Desojo, 2011; Scheyer et al., 2014; Cerda et al., 2018). Both, aetosaurs and phytosaurs, preserve a diploe structure in their osteoderms (Scheyer

et al., 2014). The main difference between the two clades is visible in the construction of the cortices: in phytosaurs (except for Phytosauria indet. from Germany and the *Pseudopalatus* sp. from the USA; Scheyer et al., 2014) the internal and external cortex is built from parallel-fibred bone and is highly vascularized with clearly visible and countable growth marks (LAGs, zones and annuli); whereas in aetosaurs the internal (basal) cortex consists also of parallel-fibred bone, but the external cortex is made of lamellar bone. Depending on the aetosaurian taxon sampled, the osteoderms contain also woven-fibred bone (Cerda & Desojo, 2011; Cerda et al., 2018). Moreover, vascular density is considerably lower in aetosaur osteoderms when compared to phytosaur osteoderms (Cerda & Desojo, 2011; Scheyer et al., 2014).

Seitz (1907) was the first who studied and figured femoral histology of the phytosaur *Belodon* (= *Nicrosaurus*) *kapffi* from the Stubensandstein Formation from Stuttgart. De Ricqlès et al. (2003) examined a total of seven long bones (femora, humeri and radii) of five taxa: two phytosaurs Phytosauria indet. and *Rutiodon* sp., and three aetosaurs *Stagonolepis* (= *Calyptosuchus*) sp., *Desmatosuchus* sp., and *Typothorax* sp., all originating most probably from the Placerias Quarry in Arizona, USA. Hoffman et al. (2019) sampled a partial radius and a fragmentary fibula of the aetosaur *Coahomasuchus chathamensis* originating from a locality in North Carolina, USA. Butler et al. (2019) studied a single femur of the phytosaur *Mystriosuchus steinbergeri* from the marine deposits from Austria. Recently, Heckert et al. (2021) studied a pathological femur of *Smilosuchus gregorii* from the USA, Arizona. Most recently, Ponce et al. (2022) studied a total of five long bones (femora, humeri, tibia) belonging to two individuals of *Aetosauroides scagliai* from Argentina. The main results of the available histological studies performed on aetosaurs and phytosaurs long bones are listed in table 1. In summary, all these samples show the deposition of fibro-lamellar bone (FLB) in the inner cortex with a switch to lamellar-zonal bone (LZB) in the outer cortex, the presence of an external fundamental system (EFS), and alternating distinct growth marks in form of zones, annuli and lines of arrested growth (LAGs; table 1) of both phytosaurs and aetosaurs. Due to a different origin of limb bones and osteoderms (periosteal bones vs. dermal bones), a direct comparison of the growth record of those elements is not advisable (Klein et al., 2009; Hayashi et al., 2012).

Aim of study

Microanatomy, long bone histology and growth pattern of the semi-aquatic phytosaur *Parasuchus* cf. *arenaceus* and the terrestrial aetosaur *Stagonolepis olenkae* from the Krasiejów locality are studied for the first time. Further on, femoral histology of the similarly aged (Norian) but geographically distinct phytosaur *Nicrosaurus* sp. from the German Heslach locality is studied as well. Results (i.e., growth pattern) are compared to published growth record data of aetosaurs and phytosaurs from various global localities. Moreover, the growth pattern of a temnospondyl amphibian and a dinosauromorph from Krasiejów are also compared, to test if the environmental factors had an influence on the growth pattern of those vertebrates.

Material and methods

Material

One humerus and three femora of *Parasuchus* cf. *arenaceus* from the Late Triassic (Norian) of Krasiejów are studied (table 2, figs 1–2). Humerus UOPB 00145 measures 19.4 cm (fig. 2A–D), which is 89% of the largest known

TABLE 1 Main results of the available histological studies performed on aetosaurs and phytosaurs long bones

Taxon	Provenance	Element	Bone histology	Growth rate and growth cycle count	Reference
Aetosauria					
Desmatosuchus sp.	USA, Arizona	proximal humerus	The inner cortex consists well-vascularized FLB consisting of both, woven and lamellar components; external cortex is built of more LZB and the alternating vascular zones are separated by distinctive avascular annuli associated with a LAG that can be accompanied by multiple rest lines; the external most cortex becomes lamellar and avascular; remodelling by secondary osteons	High initial growth rate for the inner cortex and a moderate growth rate for the outer cortex, 15–16 growth	de Ricqlès, Padian & Horner (2003)
Desmatosuchus sp.	USA, Arizona	distal radius	Not sampled at the midshaft plane; inner cortex consists of a homogenous bone matrix with vascularized zones separated by (almost) avascular, thin annuli with associated LAGS; towards the external cortex the zones become thinner and in the external most cortex they are almost avascular; at least 10 cycles are visible in the cortex exclusive of the very numerous LAGS in the most external cortex; remodelling by secondary osteons	Low growth rate, with a possible higher growth rate earlier in the ontogeny; >10 LAGS	de Ricqlès, Padian & Horner (2003)
Calyptosuchus (‘*Stagonolepis*’) sp.	USA, Arizona	femur	Inner cortex consists of highly vascular FLB with woven bone component and continues with an alternation with avascular, more lamellar tissue associated with at least one LAG; towards the outer cortex the tissue becomes more LZB with sequence of alternating thin and less vascularized zones and annuli; the external most cortex is lamellar and poorly vascularized, cortex stratified by multiple LAGS with no indication for an EFS;	High growth rate at the beginning and continues with low to very low growth rate; at least 10 LAGS	de Ricqlès, Padian & Horner (2003)

Typothorax sp.	USA, Arizona	proximal humerus	Longitudinal section and no information about the growth pattern visible	No estimation of the growth rate or growth cycle count are possible	de Ricqlès, Padian & Horner (2003)
Typothorax sp.	USA, Arizona	distal radius	The cortex is moderately vascularized and stratified by 10–12 LAGs resembling a LZB type; the outermost cortex is lamellar and poorly vascularized, with numerous LAGs preserved, however sheets of FLB with primary osteons oriented longitudinally and radially is also preserved; moderate remodelling by mostly circular erosion rooms and scattered secondary osteons sometimes reaching into the deep cortex	Low growth rate, 10–12 LAGs	de Ricqlès, Padian & Horner (2003)
Coahomasuchus chathamensis	USA, North Carolina	fragmentary radius	Inner cortex consists of woven-fibered bone (until the 1st LAG) and continues with progressively thinner layers of PFB; vascularity decreases towards the cortex surface; few scattered secondary osteons in the inner cortex	Fast growth rate, 7 LAGs, EFS	Hoffman, Heckert & Zanno (2019)
Coahomasuchus chathamensis	USA, North Carolina	fragmentary fibula	Innermost cortex consists of highly vascularized woven-fibered bone; the outer cortex consists of less vascularized PFB; dense remodelling by secondary osteons in the inner cortex	Fast growth rate, 7 LAGs, EFS	Hoffman, Heckert & Zanno (2019)
Aetosauroides scagliai	Argentina	humerus, femur; PVL 2073	Both elements consist of highly vascularized FLB in the inner and middle region preserving more wove bone and towards the outer cortex PFB; entire cortex stratified by LAGs with various spacing	Fast growth rate for the inner cortex and slower growth rate for the outer cortex, 10 LAGs, no EFS	Ponce, Desojo & Cerda (2022)

Aetosauroides scagliai	Argentina	humerus, femur, tibia; PVL 2052	Cortices of the femur and tibia highly vascularized, the humerus is low vascularized; all elements grow with FLB and towards the outer cortex the deposition of PFB is more pronounced; entire cortex stratified with LAGs with various spacing	Fast growth rate for the inner cortex and slower growth rate for the outer cortex, 4–5 LAGS (femur and tibia) and 8 LAGs (humerus), EFS only in femur and tibia	Ponce, Desojo & Cerda (2022)
Phytosauria					
Belodon (= *Nicrosaurus*) *kapffi*	Germany	femur	Prominent concentric growth rings reaching far into the deeper cortex with characteristic Harversian canals embedded with no order, the vascularization is present by primary vascular canals and less abundant radial canals building anastomoses; towards the inner cortex the concentric lines are becoming unorganized and larger erosion cavities are occurring in the innermost section portion; no further description of the tissue, no description of the vascular density, no description of the remodelling	No estimation of the growth rate and growth mark count was proposed and the figures are not sufficient to make an estimation approach	Seitz (1907)
Rutiodon sp.	USA, Arizona	proximal femur	Internal cortex consists of highly vascularized FLB but with a poorly developed woven component; the external cortex consists of PFB with cyclical deposition of growth marks (zones, annuli and LAGs); the annuli associated with LAGs are intercalated with thinner and less vascularized zones built of PFB; two outermost zones contain again woven component; flattened erosion cavities preserved in the inner cortex; locally scattered secondary osteons occur	Fast-growing internal cortex and a slowed-down growth rate for the outer cortex; 13–16 LAGs; no EFS	de Ricqlès, Padian & Horner (2003)

Phytosauria indet.	USA, Arizona	proximal femur	The internal cortex remodelled and the external cortex consists of LZB with a PFB component; a sequence of nearly avascular annuli built of lamellar tissue is associated with one to several LAGs, separated by vascularized, thicker zones build of lamellar periosteal tissue and some with woven bone; remodelled internal cortex with scattered, large secondary osteons	External cortex deposited at a moderate to low growth rate; At least 10 LAGs; no EFS	de Ricqlès, Padian & Horner (2003)
Mystriosuchus steinbergeri	Austria	femur	Cortex consists of LZB tissue with low vascularized zones built of PFB separated by LAGs; larger erosion cavities and secondary osteons, locally more extensively remodelled	Low bone deposition speed, 8 LAGs, no EFS	Butler et al. (2019)
Smilodon gregorii	USA, Arizona	humerus	Presence of woven bone and lamellar bone stratified with numerous LAGs; no further description of the tissue, no description of the vascular density, no description of remodelling	Low growth rate	Heckert, Viner & Carrano (2021)

Abbreviations: EFS = external fundamental system; FLB = fibro-lamellar bone; LAG = line of arrested growth; LZB = lamellar-zonal bone; PFB = parallel-fibered bone.

TABLE 2 Measurements of the sectioned long bones. Please note that, based on a complete specimen of *Parasuchus hislopi* from India, the humerus femur ratio reveals that humerus UOPB 00145 and femur UOPB 00143 correspond to the same size class when considering total body length of the individual. The humerus vs. femur range from *Stagonolepis robertsoni* reveals that the size range of the sampled humeri fits to the calculated body size revealed for the femora of the *S. olenkae*. Based on calculated maximal size and tissue all here studied individuals are regarded as adults

Specimen number	Element	Taxon	Total length (cm)	Proximal width (cm)	Distal width (cm)	Midshaft width (cm)	Total (%)	Visible growth cycles	Compactness with medullary cavity (bone %)	Compactness without medullary cavity (bone %)
UOBS 03370	femur	*Parasuchus* cf. *arenaceus*	39	8.4	–	4	100	6	90	99
UOPB 01026	femur	*Parasuchus* cf. *arenaceus*	37	8	8.2	3.5	95	6	80	96
UOPB 00143	femur	*Parasuchus* cf. *arenaceus*	25	6.1	4.7	3.3	64	5	66	97
SMNS 4381/2	femur	*Nicrosaurus* sp.	29.5	8.3	–	4.2	89	4	74	84
UOPB 00145	humerus	*Parasuchus* cf. *arenaceus*	19.4	6.9	5.3	2.1	86		79	98
UOPB 00123	femur	*Stagonolepis olenkae*	37	11.2	7.7	6.6	100	–	93	95
UOPB 00122	femur	*Stagonolepis olenkae*	33	9.6	9.6	6.5	89	–	97	97
UOPB 00137	humerus	*Stagonolepis olenkae*	24	12.4	–	3.6	100	2	93	–

UOBS 02828	humerus	*Stagonolepis olenkae*	23.8	12.2	–	3.4	99	3	95	–
UOPB 00121	humerus	*Stagonolepis olenkae*	22.8	11.3	7.1	2.8	95	4	88	98
UOPB 00142	humerus	*Stagonolepis olenkae*	22.6	10.9	7.6	3.1	94	5	87	–
UOPB 00136	humerus	*Stagonolepis olenkae*	–	–	6.7	2.5	?92	6	80	97
UOBS 01906	humerus	*Stagonolepis olenkae*	22.1	11.2	7	3.1	92	3	76	95
UOBS 02363	humerus	*Stagonolepis olenkae*	21.9	11.8	7	3	91	2	79	92
UOBS 02496	humerus	*Stagonolepis olenkae*	21.7	11.1	6.5	3	90	3	78	95
UOPB 00120	humerus	*Stagonolepis olenkae*	21.7	10.4	7.3	2.8	90	4	85	94
UOPB 00135	humerus	*Stagonolepis olenkae*	21.6	10.7	5.7	2.8	90	4	88	94

FIGURE 1 Morphology of the studied femora of the phytosaurs *Parasuchus* cf. *arenaceus* UOPB 00143 (A-D), and *Nicrosaurus* sp. SMNS 4381/2 (E-G), and the aetosaur *Stagonolepis olenkae* UOPB 00122 (H-K). A, E and H in lateral view; B, F and I in medial view; C, G and J in proximal view; D and K in distal view. The arrows point to the histological plane of sectioning. Scale bars represent 5 cm for each specimen.

humerus from Krasiejów (ZPAL III 1516, 20.7 cm; Kimmig, 2013). As the material from Krasiejów is disarticulated and no proxy for the humerus to femur ratio is known, we used the known ratio of a closely related species and articulated specimen, *Parasuchus hislopi* from India (ISI R 42; femur length = 24 cm; humerus length = 18.2 cm; Chatterjee, 1978). This ratio reveals that humerus UOPB 00145 (19.4 cm) would correspond to a femur with a length of around 25.6 cm. Following that assumption, the sampled humerus UOPB 00145 and the femur UOPB 00143 would correspond to a similar size class (table 2). The sampled femora of *P.* cf. *arenaceus* represent a growth series ranging from 25 cm to 39 cm. This translates to 64% to 100% when considering the length of the largest known femur from Krasiejów (UOBS 03370, 39 cm; EMT, 2021, pers. obs.). The here studied femoral section of the phytosaur *Nicrosaurus* sp. originating from the German Late Triassic (Norian) locality (SMNS 4381/2; approx. length 29.5 cm; fig. 1E-G) is 89% size of the largest known femur of this taxon (SMNS 4381/1, 33 cm; EMT, 2021, pers. obs.; table 2).

From the aetosaur *Stagonolepis olenkae* from the Late Triassic (Norian) of Krasiejów, ten humeri (21.6 cm to 24 cm) and two femora (33 cm and 37 cm) were sampled (fig. 1H–K). The size of the humeri corresponds to 90% to 100% of the largest known humerus length from Krasiejów (UOPB 00137, 24 cm; EMT, 2021, pers. obs.; table 2), while the femur length corresponds to 89% to 100% of the largest known femur from Krasiejów (UOPB 00123, 37 cm; EMT, 2021, pers. obs.; table 2). Thus, all sampled bones of aetosaurs represent the upper size range. Since the aetosaur material from Krasiejów preserves only disarticulated specimens, no ratios for e.g., humerus vs. femur can be given, too. Based on the closely related *S. robertsoni* from Scotland, the humerus vs. femur ratio is 0.63 (Walker, 1961). Using this ratio, the largest preserved

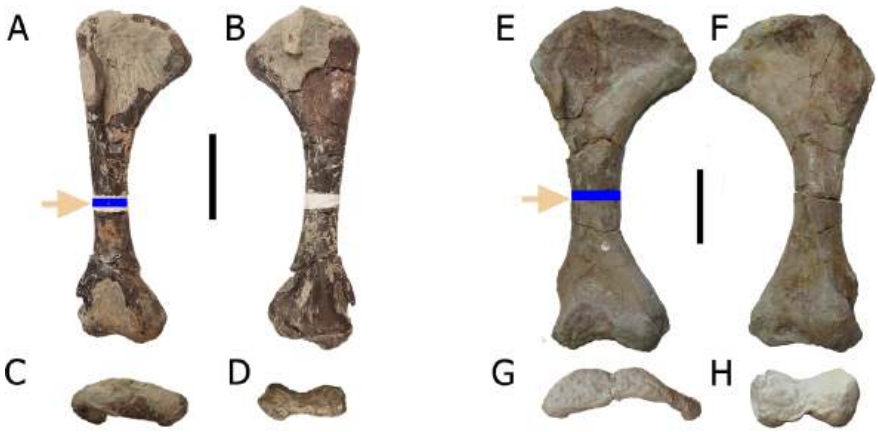

FIGURE 2 Morphology of the studied humeri of the phytosaurs *Parasuchus* cf. *arenaceus* UOPB 00145 (A-D), and the aetosaur *Stagonolepis olenkae* UOBS 01906 (E-H). A and E in ventral view; B and F in dorsal view; C and G in proximal view; D and H in distal view. The arrows point to the histological plane of sectioning. Scale bars represent 5 cm for each specimen.

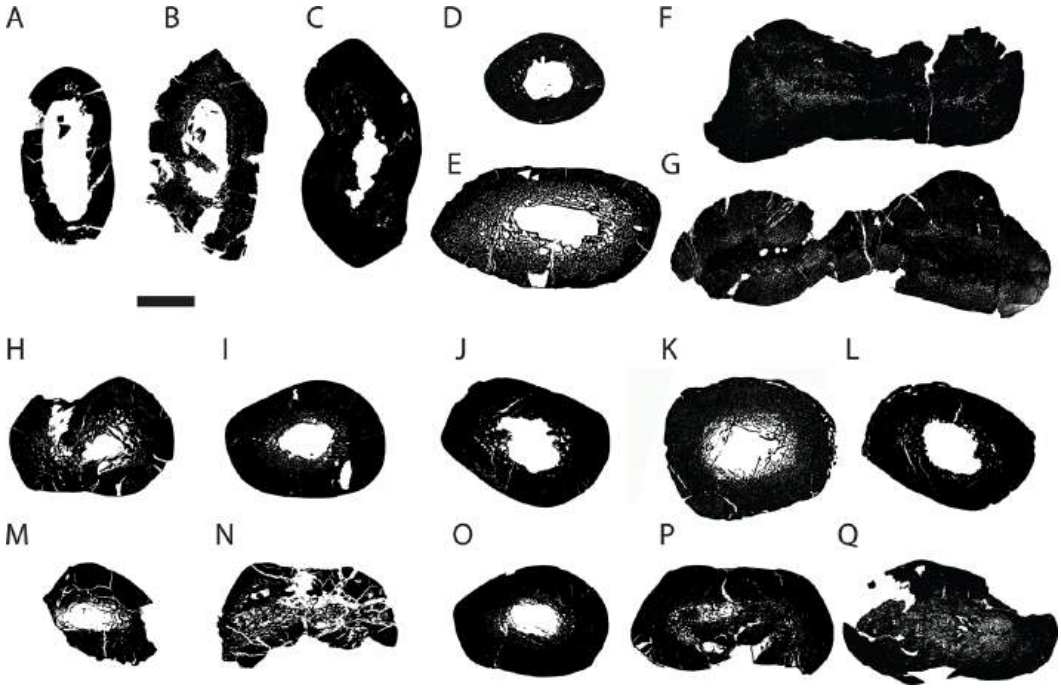

FIGURE 3 Mid-diaphyseal cross-sections of all sectioned specimens showing the bone microanatomy of the phytosaurs *Parasuchus* cf. *arenaceus* femora (A: UOPB 00143, B: UOPB 01026, C: UOBS 03370 and humerus (D: UOPB 00145), and *Nicrosaurus* sp. femur (E: SMNS 4381/2), the aetosaur *Stagonolepis olenkae* femora (F: UOPB 00122, G: UOPB 00123) and humeri (H: UOPB 00135, I: UOPB 00120, J: UOBS 02496, K: UOBS 02363, L: UOBS 01906, M: UOPB 00136, N: UOPB 00142, O: UOPB 00121, P: UOBS 02828, and Q: UOPB 00137). Taxa are arranged accordingly to their bone length. Scale bar represents 1 cm for each specimen.

femur (UOPB 00123, 37 cm) of *S. olenkae* sectioned here would correspond to a humerus of approx. 23 cm and the second femur sampled (UOPB 00122, 33 cm) would correspond with a humerus of approx. 21 cm. Thus, both femora fit to the size class of the sampled humeri.

All histological samples were taken from diagnostic humeri and femora (table 2, figs 1A–K, 2A–H). Before sampling, the taxonomical affiliation of the sampled bone either to aetosaur or to phytosaur, respectively was assured. The humeri of aetosaurs and phytosaurs can be easily distinguished: a phytosaurian humerus has a very straight medial edge of the shaft which forms almost a straight line with the proximal and distal head (fig. 2A–B, E–F; Kimmig, 2013). On the contrary, aetosaurian humeri possess a transversely wider expanded proximal head and show a more pronounced deltopectoral crest that expands laterally (Walker, 1961; Nesbitt, 2011; Roberto-Da-Silva et al., 2014; Dróżdż, 2018; fig. 2E–F). The femora of aetosaurs can be well differentiated from phytosaurs because they

TABLE 3 Thickness of zones and annuli in the phytosaurs *Parasuchus* cf. *arenaceus* and *Nicrosaurus* sp. (cycle number vs. cycle thickness)

Total length (cm)		**25**	**37**	**39**	**29.5**	**19.4**
Element		**femur UOPB 00143**	**femur UOPB 01026**	**femur UOBS 03370**	**femur SMNS 4831/2**	**humerus UOPB 00145**
1st	zo	–	23	–	35	22
	an	12	19	39	12	3
2nd	zo	9	10	20	23	21
	an	12	4	6	5	5
3rd	zo	7	5	3	5	8
	an	9	9	2	12	6
4th	zo	9	3	2	2	4
	an	5	5	16	6	4
5th	zo	9	11	2	–	12
	an	28	4	8	–	6
6th	zo	–	2	2	–	6
	an	–	5	–	–	3

Colours: green = zone thicker than the annulus, yellow = almost no variation in the thickness of the zones or annuli; red = annulus thicker than the zone. Abbreviations: zo = zone, an = annulus. The cycle count starts with the 1st cycle being in the innermost cortex (towards the medullary cavity) with the subsequently numbered cycles continuing towards the outer cortex (towards the bone surface)

TABLE 4 Thickness of zones and annuli in the aetosaur *Stagonolepis olenkae* (cycle number vs. cycle thickness)

Total length (cm)		21.6	21.7	21.7	21.9	22	22.1*	22.6	22.8	23.8*	24*
Element		UOPB 00135 humerus	UOPB 00120 humerus	UOBS 02496 humerus	UOBS 02363 humerus	UOBS 01906 humerus	UOPB 00136 humerus	UOPB 00142 humerus	UOPB 00121 humerus	UOBS 02828 humerus	UOPB 00137 humerus
1st	zo	40	7	32	–	19	40	37	–	19	17
	an	6	4	10	57	21	8	4	6	8	10
2nd	zo	29	21	26	14	19	30	16	19	16	33
	an	6	14	13	29	16	3	4	8	8	40
3rd	zo	6	7	5	–	9	2	3	26	10	–
	an	8	16	14	–	16	1	10	6	39	–
4th	zo	2	7	–	–	–	4	6	19	–	–
	an	3	24	–	–	–	2	8	16	–	–
5th	zo	–	–	–	–	–	2	6	–	–	–
	an	–	–	–	–	-	2	6	–	–	–
6th	zo	–	–	–	–	–	2	–	–	–	–
	an	–	–	–	–	–	4	–	–	–	–
Estimated cycles**		4	4	5	6	6	6	5	4	5	5

*estimated total bone length, **the visible growth cycles plus the estimated resorbed cycles.

Colours: green = zone thicker than the annulus, yellow = almost no variation in the thickness of the zones or annuli, red = annulus thicker than the zone. Abbreviations: zo = zone, an = annulus. The cycle count starts with the 1st cycle being in the innermost cortex (towards the medullary cavity) with the subsequently numbered cycles continuing towards the outer cortex (towards the bone surface).

are robustly built, elongated and show almost no torsion between the proximal and the distal head (fig. 1H–K). In contrast, the femora of phytosaurs are more slender and show a prominent sigmoidal curvature between the proximal and distal heads (fig. 1A–B), which is often visible in aquatic animals (Kimmig, 2013; EMT, 2021, pers. obs.).

Methods

All bone samples were processed into standard petrographic thin-sections in the laboratory of the Institute of Geosciences (IGPB) at the University of Bonn, Germany. All limb bones were sectioned transversely at the midshaft plane according to the technique described in Klein & Sander (2007). For grinding and polishing of the thin-sections wet silicon carbide (SiC) grinding powders with grit sizes of 600 and 800 were used. The osteohistological analysis was performed with a Leica DM LP polarizing light microscope (with objectives of 1.25×, 4×, 10× and 20× magnification) and the photographs were taken with a Leica DFC 420 camera attached to the microscope. The overview pictures in polarized light were stitched with the *AutoStitch* software (http://www.autostitch.net). The cross-sections for microanatomical analyses were scanned with an Epson Perfection 750V PRO scanner.

Pictures of cross sections were transformed to black (compact bone) and white (cavities) pictures to measure bone compactness. The pixel counting software then was measuring white and black pixels (©Peter Göddertz, IGPB), resulting in a ratio of compact bone to cavities (table 2, fig. 3A–Q). The compactness was measured for the complete section, including the medullary cavity and/or region and also by excluding the latter and measuring only the cortex (table 2). The histological nomenclature follows Francillon-Vieillot et al. (1990).

Growth mark count was performed under polarized light in which the differences in tissues organization of the alternating growth marks, i.e., zones and annuli, were best visible. A growth mark was identified as belonging to an annual cycle when it was followed nearly continuous over the entire cross section. Contrary, sub-cycles are defined as thin layers of high organized tissue, resembling the characteristics of annuli, that are locally restricted. The relative thickness of the zones and annuli (tables 3–4) was measured, if possible due to preservation, at the same bone area: on the posteromedial side for the femora (table 3) and on the dorsal side in the humeri (table 4).

Results

Microanatomy and histology

Parasuchus cf. *arenaceus*. All studied cross sections of femora are elliptical (fig. 3A-B), except for the large femur (UOBS 03370; fig. 3C), which was dorsoventrally compacted. The humerus section is more rounded in cross section (fig. 3D). All sections share a central, free medullary cavity, which is largest in the smallest femur (UOPB 0143, 25 cm) and smallest in the largest femur (UOPB 03370, 39 cm) (fig. 3C). The values of the bone compactness measured for the entire cross section range from 66 to 90% for the femora and it is 79% for the humerus (table 2). Based on the microanatomical analysis performed, those specimens show a tendential bone mass increase with increasing size. The cortex compactness (excluding the medullary cavity) is very high in all four specimens ranging between 96% to 99% (table 2), indicating a low vascular density. The medullary cavity is lined by a thin layer of endosteal bone in all four samples (fig. 4A–C). The primary periosteal cortex is built by parallel-fibred bone with varying

degrees of collagen fibres organization in all three femora and the humerus (fig. 4D). In the femora, the vascular density is low to moderate (table 2, see bone compactness) and only the humerus is somewhat higher vascularized. Femora and humerus, show small simple vascular canals and primary osteons, the latter are more numerous but small, too. They are mostly longitudinal to reticular in shape and sometimes arranged in a plexiform system. Simple vascular canals are most numerous in the outermost cortex, whereas primary osteons are preserved throughout the entire cortex. In the humerus, the simple vascular canals are smaller and more abundant than in the femora. In the outer cortex of every specimen, the simple vascular canals are arranged in rows. Radial primary osteons occur on the medial and lateral side in the femoral sections. Vascular canals are largely restricted to the zones whereas annuli are usually avascular. Osteocyte lacunae are equally numerous throughout the cortex of all sections. They are irregular in size and shape and lack canaliculi. Sharpey's fibres are visible only in the outermost cortex of femur UOPB 01026.

The degree of remodelling in form of erosion cavities in the inner cortex and secondary osteons scattered into the primary cortex varies in the samples with no order along size. All phytosaur femora samples display small, nearly closed secondary osteons which are restricted to the inner cortex (UOPB 00143 and UOBS 03370; fig. 3A, C), except for the middle-sized femur (UOPB 01026) where they are numerous and reach far into the outer cortex (fig. 3B). The humerus UOPB 00145 shows only few, small, scattered erosion cavities restricted to the innermost cortex and no secondary osteons are observed in this specimen (fig. 4A–C). This fits with the low degree of remodelling observed in the smallest sampled femur (UOPB 00143) where only the lateral bone side shows few, scattered, small erosion cavities. In femur UOPB 01026 numerous, large erosion cavities and secondary osteons occur in the innermost cortex close to the boundary with the medullary cavity. In the middle and outer cortex, only secondary osteons occur and they are smaller and scattered. This specimen contains a well demarked and distinct concentric layer of densely packed erosion cavities and endosteal bone, resembling the content of a medullary region. However, this layer is above the thin layer of endosteal bone lining the medullary cavity i.e., outside the endosteal domain. In the largest specimen (UOBS 03370), small erosion cavities are scattered throughout the inner cortex but are less abundant, when compared to UOPB 01026.

Nicrosaurus sp. The sampled femur of *Nicrosaurus* sp. (SMNS 4381/2; table 2, fig. 4E–H) has an elliptical cross section (figs 3E, 4E). The central medullary cavity is in comparison to that of the above-described specimens relatively small (table 2, fig. 4E). It is lined by a thin layer of endosteal bone (fig. 4F). Bone compactness for the entire femur cross section is 74% and the cortex compactness (excluding the medullary cavity) is 84 % (table 2). The primary cortex consists of parallel-fibred bone with varying degree of collagen fibres organization (fig. 4G). The vascular density is moderate and is represented by longitudinal to reticular simple vascular canals and primary osteons. In the outermost cortex, simple canals are arranged in rows (fig. 4G–H). On the medial and lateral side, the simple vascular canals become radial. Numerous primary osteons occur throughout the cortex and they are mostly longitudinally oriented. Osteocyte lacunae are very numerous and are represented equally throughout the cortex. They are irregular in size and shape and show well developed canaliculi. Sharpey's fibres are not visible in this section.

The central medullary cavity is surrounded by a broad medullary region, both making 66% of the entire section. Their boundary is clear at the dorsal side where a thin layer

of endosteal bone separates them, but both merge into each other at the sides. Towards the primary cortex the medullary region is also not well delineated, forming around its outer periphery a perimedullary region where erosion cavities and endosteal bone

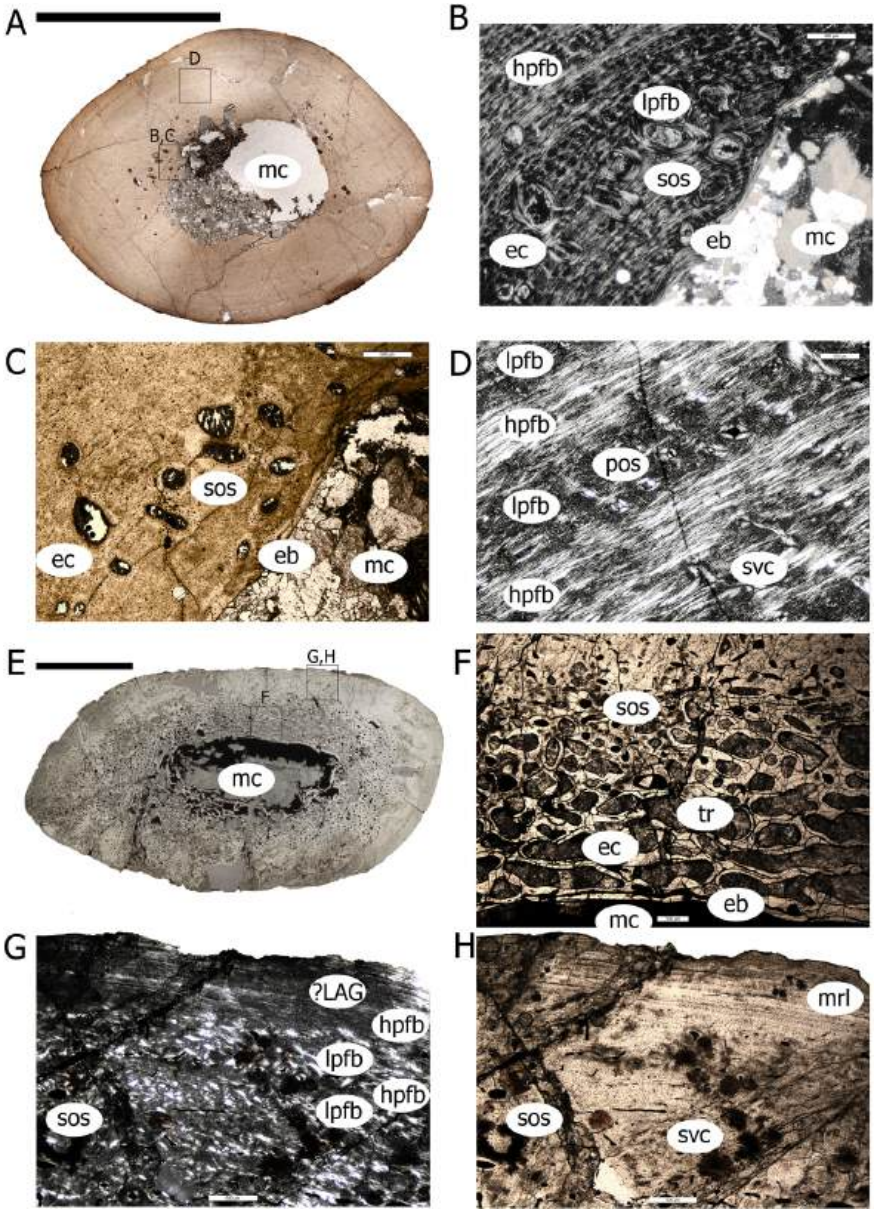

FIGURE 4 Histological growth of the phytosaurs *Parasuchus* cf. *arenaceus* on the example of the humerus UOPB 00145 (A-D) and the *Nicrosaurus* sp. femur SMNS 4381/2. Pictures A, C, E-F and H were taken under normal transmitted light and pictures B, D and G were taken under polarized light. Scale bars represent 1 cm for specimens A and E, 500 micrometres for specimens B-C, F-H and 100 micrometres for specimen D. Abbreviations: eb = endosteal bone, ec = erosion cavity, hpfb = higher organized parallel-fibered bone, LAG = Line of Arrested Growth, lpfb = lower organized parallel-fibered bone, mc = medullary cavity, mrl = multiple resting lines, pos = primary osteon, sos = secondary osteon, svc = simple vascular canal, tr = trabecular region.

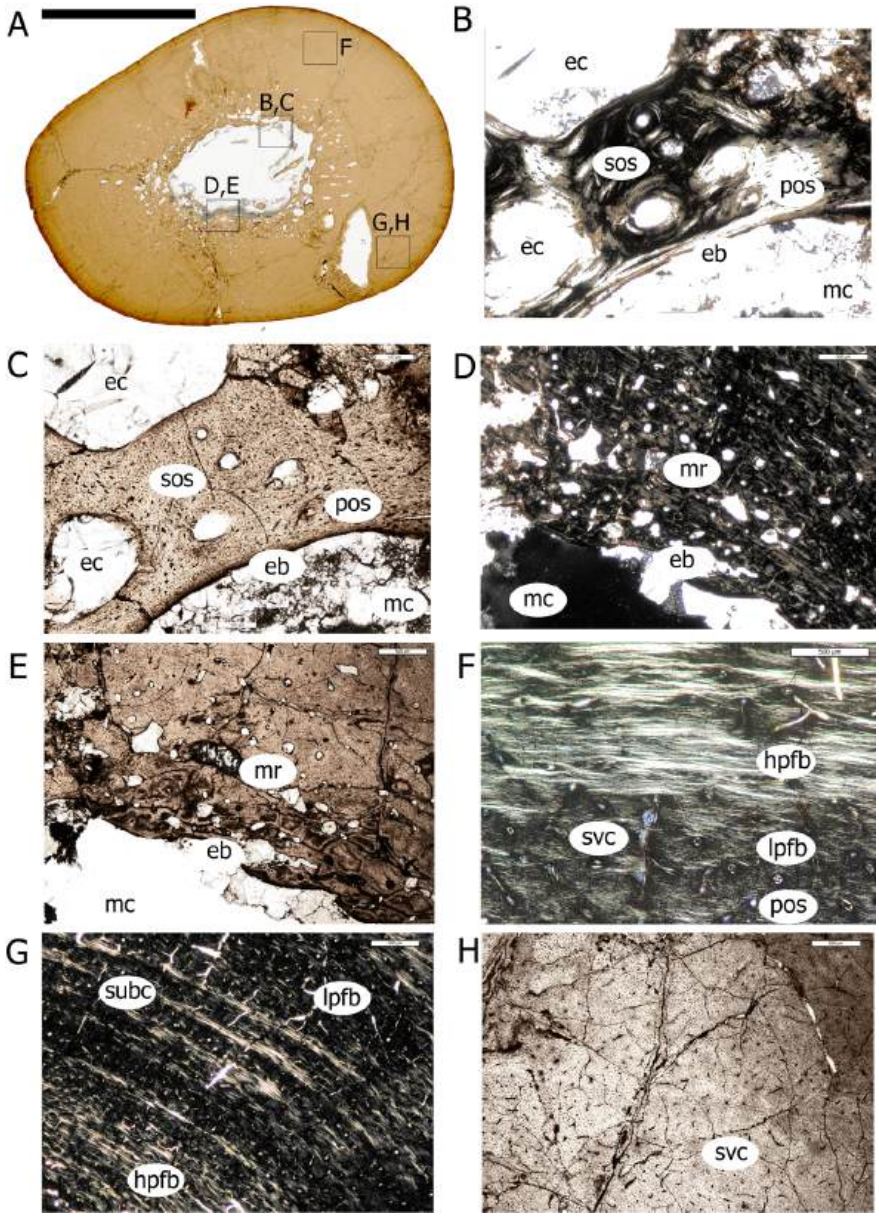

FIGURE 5 Histological growth of the aetosaur *Stagonolepis olenkae* on the example of the humerus UOPB 00120 (A-H). Pictures A, C, E and H were taken under normal transmitted light and pictures B, D, and F-G were taken under polarized light. Scale bars represent 1 cm for specimen A, 100 micrometres for specimens B-C, and 500 micrometres for specimens D-H. Abbreviations: eb = endosteal bone, ec = erosion cavity, hpfb = higher organized parallel-fibered bone, lpfb = lower organized parallel-fibered bone, mc = medullary cavity, mr = medullary region, pos = primary osteon, sos = secondary osteon, subc = sub cycles, svc = simple vascular canal.

are intermixed with scattered secondary osteons and primary cortex. Along the boundary to the medullary cavity, the medullary region consists of large rectangular shaped (dorsoventrally aligned) erosion cavities, forming a trabecular structure (fig. 4F). Towards

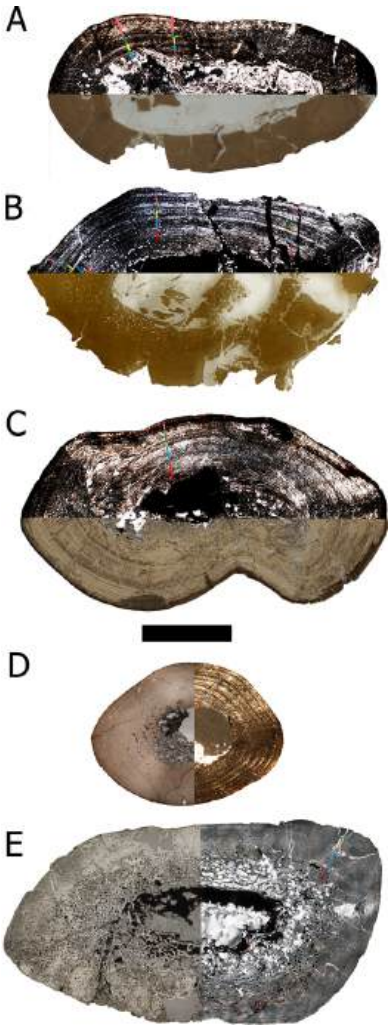

FIGURE 6 Growth pattern of the sectioned phytosaurs *Parasuchus* cf. *arenaceus* femora (A: UOPB 00143, B: UOPB 01026, C: UOBS 03370) and humerus (D: UOPB 00145) and *Nicrosaurus* sp. (E: SMNS 4381/2). Half of the picture is taken under normal transmitted light and the other picture half is taken under polarized light. Please note, that the normally transmitted picture does not show informative histological features. The coloured bars show preserved and counted cycles (zone and annulus). Specimen A preserves five growth cycles, specimen B, C and D preserve six growth cycles, and specimen E preserves four growth cycles. Taxa are arranged accordingly to their bone length. Scale bar represents 1 cm for each specimen.

the outer cortex the erosion cavities become round and are getting continuously smaller.

Stagonolepis olenkae. The aetosaur femora have an irregular but elongated cross-sectional shape (figs 3F–G, 5A). The humeri are roundish to oval (fig. 3H–K, N–Q), except for the dorsoventrally compacted specimens UOBS 02828 and UOPB 00142 (fig. 3L–M). When not compacted due to preservation, the centrally positioned medullary cavity is in all specimens surrounded by a thin layer of endosteal bone (fig. 5A–E). Bone compactness for the entire cross section ranges from 93% to 95% for the femora and between 76% to 95% for the humeri (table 2). The cortex compactness (excluding the medullary cavity) ranges between 95% to 97% for the femora, and it is between 92% to 98% for the humeri (table 2). The primary cortex is made of parallel-fibred bone tissue deposited in different degree of collagen fibres organization (fig. 5F–G). All sections show a moderate vascular density (table 2). The simple vascular canals and primary osteons are mostly longitudinal to reticular in shape. Primary osteons occur mostly in the outer cortex (fig. 5B–H). Although all humeri are of a similar size range (table 2), the number of vascular canals in the humeri is the lowest in the upper bone size range. Osteocyte lacunae are very prominent in all studied specimens. They are irregular in shape, small but numerous and are distributed throughout the entire cortex. Very short fibres are documented in the humeri UOBS 01906 and UOBS 02363, in which they are occurring sporadically in the outer cortical surface.

The broadness of the medullary region that surrounds the medullary cavity varies from narrow (e.g., UOPB 00120, UOPB 00121 and UOPB 00136) to very thick (e.g., UOBS 02363). A correlation between size of the medullary region and bone length is not identified. The erosion cavities are irregularly shaped in the

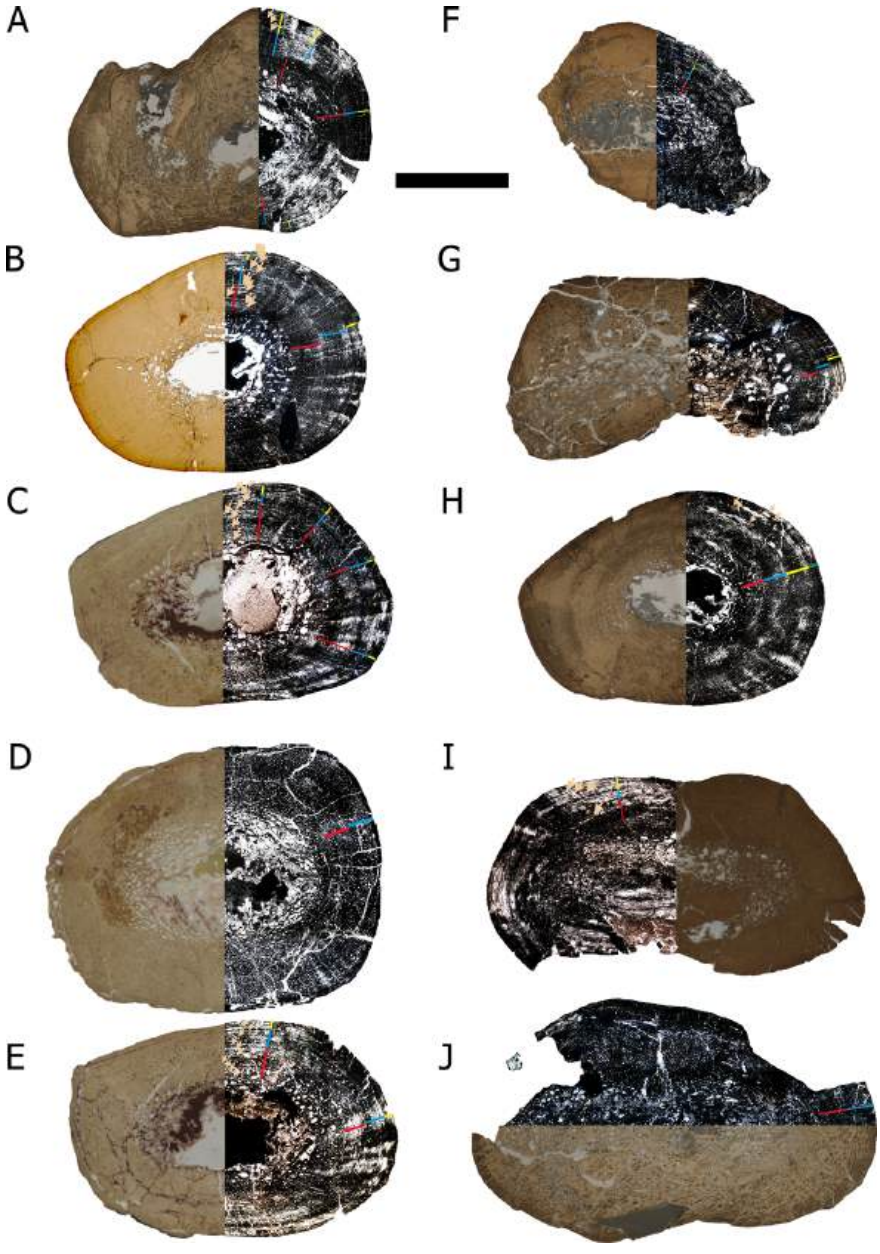

FIGURE 7 Growth pattern of the sectioned aetosaur *Stagonolepis olenkae* humeri (A: UOPB 00135, B: UOPB 00120, C: UOBS 02496, D: UOBS 02363, E: UOBS 01906, F: UOPB 00136, G: UOPB 00142, H: UOPB 00121, I: UOBS 02828, and J: UOPB 00137). Half of the picture is taken under normal transmitted light and the other picture half is taken under polarized light. Please note, that the normally transmitted picture does not show informative histological features. The coloured bars show preserved and counted cycles (zone and annulus). Specimen A-B and H preserve four growth cycles, specimen C, E, G, and I preserve three growth cycles, specimen D and J preserve two growth cycles and specimen F preserved six growth cycles. The arrows in specimens A-C, E, and H-J indicate sub-cycles. Humeri are arranged accordingly to their bone length. Scale bar represents 1 cm for each specimen.

inner medullary region and become smaller and round towards the outer cortex. The two femora (UOPB 00122 and 00123) are almost completely remodelled by secondary osteons, leaving only a small portion of primary bone visible i.e., parallel-fibred bone, in the outermost cortex.

Growth mark count and growth pattern. The entire primary cortex of *Parasuchus*, *Stagonolepis* and *Nicrosaurus* is stratified by alternating growth marks in form of zones, annuli and sometimes rest lines (tables 3–4). Zones and annuli are distinguished by a change in tissue and vascular density. Layers consisting of mostly avascular to low vascularized and high organized parallel-fibred bone partially grading into lamellar bone are interpreted as annuli. Low to moderate (in *Parasuchus*) and moderate to high (in *Nicrosaurus* and *Stagonolepis*) vascularized layers of less organized parallel-fibred bone are interpreted as zones. Under normal light growth marks are not identifiable (figs 4A, E, 5A, 6A–E, 7A–J). The distinction between zones and annuli is only possible under polarized light. Often the boundary between zones and annuli is not well delineated because they tend to merge into each other. In the aetosaurian humeri, sub-cycles are formed locally by thin layers of high organized avascular tissue (e.g., UOPB 00120, 00121, 00135, UOBS 02469, 01906; figs 5G, 6A–C, E, H–I). Multiple rest lines are documented within the annuli in all studied elements (fig. 4H). This all hampers the count of annual growth cycles. An unambiguous LAG was only identified in the outermost cortex of the *Nicrosaurus* femur (SMNS 4381/2) (fig. 4G).

In our interpretation for the current sample, an annual growth cycle consists of a zone and an annulus, which can both be followed almost all around the cross section. According to this definition, the smallest *Parasuchus* femur (UOPB 00143) shows five visible growth cycles, the middle-sized (UOPB 01026) and the largest (UOBS 03370) *Parasuchus* femur show six visible growth cycles (fig. 6A–C, table 3). The *Parasuchus* humerus shows six visible cycles (fig. 6D, table 3). Generally, the distinction of the growth cycles in the phytosaur humerus (UOPB 00145) was clearer than in the sectioned femora. The *Nicrosaurus* femur (SMNS 4381/2) shows four visible growth cycles (fig. 6E, table 3). The sampled aetosaur humeri show a slightly variable growth mark count between two and six annual growth cycles inside a small size range of 21.6 cm to 24 cm. However, bone length and number of counted cycles does not correlate (fig. 7A–J). Both aetosaur femora (UOPB 00122 and UOPB 00123) show a highly remodelled cortex making a count of annual growth cycles impossible. None of the samples document a distinct change in tissue type i.e., growth rate, for example representing the onset of sexual maturity or indicate that growth finally had ceased, as might be indicated by an EFS (Cormark, 1987).

The sequence of an annual growth cycle starts usually with a zone, except for the *Parasuchus* femora (UOPB 00143, UOBS 03370), and two *Stagonolepis* humeri (UOPB 00121, UOBS 02363). In the latter, the sequence starts with an annulus. This could either be a true signal or might be connected to the resorption of the inner growth marks. The relative thickness of an annual growth cycle is in general thicker in aetosaurs than in phytosaurs (tables 3–4). The overall thickness of growth cycles and the ratio of the thickness of zones and annuli changes from the inner to the outer cortex in both groups.

Usually, in the innermost cycles, the zone is thicker than its corresponding annulus (expect for *Stagonolepis* humerus UOBS 01906), whereas in the outermost cycles, the thickness of the annulus exceeds the thickness of the corresponding zone (tables 3–4, fig. 7E). The exception is *Stagonolepis*

humerus UOPB 00136 where the annulus and the zone are of an equal thickness in the outer cortex and *Stagonolepis* humerus UOPB 00142 where the zone is still thicker than the annulus. Thus, *Stagonolepis* humeri and the *Nicrosaurus* femur show tendentially an increasing annuli thickness towards the outer cortex. The *Parasuchus* samples do not show a trend of in- or decreasing thickness of the annuli over the zones but a rather irregular change of growth mark thickness. However, around the 3rd visible cycle in the *Parasuchus* femora the zones and annuli reach a similar thickness (table 3) and, towards the outer cortex, the zones are becoming distinctly thinner. The only exception is specimen UOPB 01026 where the zones are still thicker up to the 5th cycle than the annuli. Only in the last, the 6th cycle the annulus is becoming thicker but not as significantly as in the sections UOPB 00143 and UOBS 03370 (table 3).

In spite of a low size range, the growth pattern in the humeri of *Stagonolepis* is more variable (table 4). Six out of ten specimens start the cycle sequence with a prominently thicker zone over the annulus (UOPB 00135, 00136, 00142, 00121, UOBS 02496 and 02828). The other samples (UOBP 00120, 00142, UOBS 02496 and 01906; table 4) start with a zone with an equal thickness as the annuli. As a general trend, the annuli become thicker and zones thinner towards the outermost cortex, starting from the 3rd cycle in specimens UOPB 00120, UOBS 02496, UOBS 01906, UOBS 02828, and in specimens UOBS 02363 and UOPB 00137 already from the 2nd visible cycle (table 4). Moreover, the annuli possess sub-cycles also beginning from the 3rd cycle (UOPB 00120). Specimens UOPB 00135, UOPB 00142 and UOPB 00121 died before showing a pronounced zone thinning and annuli thickening (table 4).

In addition to the growth mark count, five stages of remodelling of the periosteal cortex are identified in the aetosaur sample that might indicate aging. However, they do not correlate with bone size in the current sample. They are: 1) the lowermost remodelling degree (UOPB 00120, UOPB 00121 & UOPB 00136); 2) low remodelling degree (UOPB 00135); 3) moderate remodelling degree (UO142, UOPB 00137, UOBS 02828); 4) high remodelling degree (UOBS 01906 and UOBS 02496); and 5) the highest remodelling degree, i.e., nearly complete remodelling of the periosteal cortex (UOBS 02363) (fig. 7D).

Discussion

Microanatomy

Bone compactness can provide information about the mode of life of an animal (Germain & Laurin, 2005; Cubo et al., 2008; Kriloff et al., 2008; Canoville & Laurin, 2009, 2010; Hayashi et al., 2012). The two major microanatomical specializations are either, a bone mass increase, observed in poorly active swimmers living in shallow marine environments, or a decrease in bone mass characterized by a more spongious organization of the cortex, observed in active swimmers usually inhabiting pelagic environments (Houssaye, 2009; Houssaye et al., 2016).

The *Parasuchus* samples from Krasiejów indicate a slight bone mass increase with increasing bone size, by reducing the size of the medullary cavity (fig. 3A–C, table 2), when compared to the microanatomy of the aetosaur sample. *Nicrosaurus* also shows a bone mass increase but differs from *Parasuchus* on the basis of the presence of a broad spongious, nearly trabecular medullary region that surrounds the medullary cavity in the latter. The last character indicates a higher degree of adaptation to an aquatic lifestyle for *Nicrosaurus*. This is, however, in contradiction with the morphological reconstruction, where

that taxon was proposed to be semi-aquatic or even secondarily terrestrial (Kimmig, 2013). The differences in femoral microanatomy between *Nicrosaurus* and *Parasuchus* can be related to phylogeny, intraspecific variability or might represent a true difference in lifestyle. However, due to a limited *Nicrosaurus* sample size, this remains highly speculative.

Stagonolepis humeri show some variation in overall bone compactness, which is mostly expressed by the varying size of their medullary cavities (fig. 3H–Q, table 2). Based on the humerus to femur proportions, known from *S. robertsoni* (Walker, 1961), the two large femora studied herein, are more compact, when compared to their corresponding humeri. The higher compactness of femora might be a result of different preservation or is related to biomechanical constraints (Kawano et al., 2016). The observed advanced remodelling in the femora, when compared to the humeri of aetosaurs, might also be related to biomechanics (Currey, 2002). Alternatively, a higher degree of remodelling can also be related to an older ontogenetic stage. The femora represent the maximal size for this group in this locality and thereby likely belonged to ontogenetically older individuals as the in size corresponding humeri. Interestingly, Ponce et al. (2022) studied two sets of corresponding femora and humeri belonging to a smaller *A. scagliai* individual (humerus: 11 cm, femur 17.6 cm), and a larger *A. scagliai* individual (humerus: 18.9 cm, femur: 27.5 cm). Their histology displayed a still preserved primary bone, and a low degree of remodelling, which is not preserved anymore in the aetosaur sample studied herein (*S. olenkae* femur: 33 cm and 37 cm; table 2).

Aetosaurs are thought to represent terrestrial herbivores and phytosaurs are interpreted as semi-aquatic to aquatic carnivores. If both groups occupied different ecological niches, this is not reflected in the microanatomy of the Krasiejów taxa, as they cover a similar compactness spectrum. A contradiction between bone compactness values and lifestyle and/or environmental interpretations was already demonstrated for other taxa, the pseudosuchian *Batrachotomus kupferzellensis* (Klein et al., 2017), but also in chelonians (Laurin et al., 2011) and extant snakes (de Buffrénil & Rage, 1993; Houssaye et al., 2010, 2013, 2014; Canoville et al., 2016). Thus, bone compactness values alone are not always a reliable source to infer the lifestyle. A compactness study preformed on one femur of the Argentinian aetosaur *A. scagliai* (74.9 %) confirmed a terrestrial lifestyle (Ponce et al., 2022). The compactness values for the *Stagonolepis* femora (table 2) show an even higher compactness, thus, can also be reconstructed as terrestrial animals.

Growth pattern comparison between the Krasiejów taxa with taxa from other localities

All three sampled taxa, the phytosaur *Parasuchus*, the aetosaur *Stagonolepis* from Krasiejów, and the phytosaur *Nicrosaurus* from Heslach, share a similar bone tissue type throughout their entire cortex, that can be summarized as LZB. For most other so far studied aetosaurs and phytosaurs (table 1; except for *Mystriosuchus* sp.), a clear change in tissue type from FLB in the inner cortex to LZB in the outer cortex was described (table 1). This change in tissue type is usually interpreted as ontogenetic change from fast growth rates in early ontogenetic stages to slower growth rates in adults and/or sexually mature individuals (de Ricqlès et al., 2003; Hoffman et al., 2019; Heckert et al., 2021; Ponce et al., 2022; table 1). Contrary, neither the taxa from Krasiejów nor the phytosaur from Heslach show woven bone in their cortex and their vascular density is moderate to low. Thus, FLB is not documented in any of our samples. A

decrease in growth rate (from moderate to low) is only observed by the increase in the thickness of annuli (tables 3–4), indicating prolonged phases of slow growth from the preserved middle cortex onwards.

The absence of fast growing, highly vascularized tissue can either be explained by the fact that the herein studied bones represent the upper size spectrum in both groups (table 2) and only late ontogenetic stages, i.e., adults had been sampled in which the change from FLB to LZB is not documented, and possibly was already resorbed by the expansion of the endosteal domain. It might also be the case, that the taxa from Krasiejów and Heslach grew in general at a lower rate, not depositing fast growing tissue even in earlier ontogenetic stages due to exogenous factors. It is possible, that due to the ontogenetically late stages the FLB was already resorbed. However, since in *Mystriosuchus* sp. from Austria, FLB was also not documented (Butler et al., 2019), it is possible, that FLB was not deposited in the studied samples, but rather became fully resorbed. In any case, the here studied individuals all represent late ontogenetic stages i.e., adult individuals, which is documented by their size range and the deposited tissue, including a certain degree of endosteal and periosteal remodelling (table 2).

The taxa from Krasiejów do not show any clear LAGs throughout their cortices nor an EFS in their outermost cortices; the phytosaur from Heslach has one LAG in its outer cortex deposited (fig. 4G). This is also contrary to the observations made in other phytosaur and aetosaur taxa where LAGs are common and an EFS is documented for several individuals (de Ricqlès et al., 2003; Hoffman et al., 2019; Butler et al., 2019; Heckert et al., 2021; Ponce et al., 2022; table 1). The two sampled *Stagonolepis* femora are nearly completely remodelled by secondary osteons, which together with their large size (table 2) indicate a late ontogenetic stage for both. However, what remains from the outermost primary cortex does not resemble an EFS. Also, the other, less remodelled samples lack an EFS or any other clear indication of a cessation in growth (i.e., avascular lamellar bone in the outer cortex). The conclusion that none of the here studied samples had stopped appositional growth and thus had not attained full size yet might be reliable. However, Late Triassic archosaurs and their kin show highly variable growth patterns and a variety of tissue types. In addition, they seem to have been highly flexible in their growth (i.e., developmental plasticity) as is also obvious from the results of the current study and seem often not to follow any clear pattern (e.g., de Ricqlès et al., 2003, 2008; Klein et al., 2017). Thus, maybe attainment of maximal body size was not always indicated by an EFS.

In former studies, growth rate was interpreted as being high in the inner cortex of most phytosaurs and aetosaurs (except for *Mystriosuchus* sp.: Butler et al., 2019), based on the deposition of FLB (i.e., highly vascularized, low organized tissue indicating fast deposition), and as low(er) in the outer cortex when tissue type had switched to LZB (de Ricqlès et al., 2003; Hoffman et al., 2019; Ponce et al., 2022; table 1). Considering the relatively high organized tissue and the low to moderate vascular density (longitudinal and reticular orientation of vascular canals), the growth rate was rather low, when compared to the growth rate in above mentioned taxa (table 1). The low growth rate applies to the samples from Krasiejów and Heslach. This is also evident from tables 3 and 4 which visualize that most of appositional growth happened during prolonged phases of slow growth. *Mystriosuchus* sp. shares with the taxa from Krasiejów and Heslach the lack of FLB and woven bone as well as the low growth rate but differs by the presence of distinct LAGs (Butler et al., 2019).

All archosaurs are likely capable of growing with woven bone/FLB (phylogenetic trajectory/precept; see Klein et al., 2017: Fig. 6) but this is not always effectuated. This is documented in modern crocodiles (e.g., Woodward et al., 2014) and possibly a similar phenomenon occurs also in the taxa from Krasiejów and Heslach as well as in *Mystriosuchus* sp. (Butler et al., 2019). Our samples confirm that the adaptational signal (i.e., exogenous factors) can be stronger than the phylogenetic signal (presence of FLB in early ontogenetic stages), as was discussed before by de Ricqlès et al. (2003, 2008). This again proofs a high developmental plasticity in early archosaurs/pseudosuchians, which might have been the key to their phylogenetic success.

Growth marks and environmental influence

The alternating growth marks in form of zones and annuli usually correspond with favourable (e.g., wet season) and unfavourable (e.g., semi-dry season) climatic conditions (Francillon-Vieillot et al., 1990). The growth record of *Stagonolepis* is more diffuse and preserves several, locally restricted sub-cycles in some humeri. The occurrence of multiple rest lines is also more common in the aetosaur than in the phytosaur samples. Fluctuating growth marks have been interpreted as evidence for unstable environmental parameters (Witzmann et al., 2012; Klein et al., 2015), which might apply to the environment in the Late Triassic of Krasiejów as well. As stated above all samples likely belong to late ontogenetic stages, i.e., adult individuals, but for none an achievement of maximal body size can be finalized. "Juvenile" tissue (i.e., highly vascularized low organized woven bone) is absent, but the onset of sexual maturity can also not be identified. Growth mark count (table 2) reveals no correlation between number of annual growth cycles and bone length (fig. 7A–J), indicating developmental plasticity. The latter is most evident by the humerus sample of *Stagonolepis*, which are all of a similar size but show a growth cycle count varying from two to six (table 4, fig. 7A–J).

The tendency of a decrease in cycle thickness from the inner to the outer cortex is however, more pronounced in *Stagonolepis* than in *Parasuchus* and *Nicrosaurus* (tables 3–4). The annuli in all three taxa increase tendentially in thickness towards the middle and outer cortex and become (partially) distinctly larger when compared to the zones (tables 3–4). Clear cessations of growth in form of LAGs are absent throughout the cortex, resulting in prolonged phases of slow growth in all individuals during which most of the recorded appositional growth was achieved.

Prolonged slow growth might be related to phylogeny (e.g., chelid turtles: Pereyra et al., 2020), endogenous, or exogenous factors (e.g., mammals: Köhler et al., 2012). If endogenous factors (e.g., diseases) are the reason usually only one individual is affected. Thus, for the prolonged slow growth phases, observed in numerous individuals of different taxa from the same locality, is best explained by exogenous factors such as climate and food availability. The pattern observed in the taxa from Krasiejów suggest a moderate climate and maybe a constant but low food availability that does not necessitate complete growth stops. A case study of wild ruminants living across different climatic zones (from polar to tropical) showed a cyclical growth (fast-growing, highly vascularized fibrolamellar bone tissue) with the deposition of LAGs (Köhler et al., 2012). This shows that the mammalian (endothermic) histological growth is not dependent on climatic conditions but rather by endogenous constraints. Hedrick et al. (2020) suggested an initial climate-induced gradient in growth patterns for ceratopsian dinosaurs, but additional sampling of closely-related taxa from geographically similar localities showed marked differences in histology, thus

these patterns were most likely phylogenetically induced.

A previous approach was performed, comparing temnospondyl amphibians of the Metoposauridae family, with a similar stratigraphic distribution (Norian/Carnian) but from geographically different localities (Europe, Asia and Africa; Teschner et al., 2020). Climate of the Maleri Formation, yielding the Indian metoposaurids, was reconstructed as warm climate with seasonal rainfalls and the living niches as ephemeral and vegetated swamps or ponds (Dasgupta et al., 2017), similarly to the reconstruction of Polish Krasiejów (Jewuła et al., 2019), however, such study is lacking for the Late Triassic lacustrine deposits of Morocco. The metoposaurids from Poland, India and Morocco showed in general a comparable histology. However, the taxon from Morocco (*Dutuitosaurus ouazzoui*) displayed distinct LAGs that were absent in the Polish *Metoposaurus* and Indian *Panthasaurus*. This could suggest a rather moderate climate, without extreme fluctuations between wet/favourable and dry/unfavourable seasons preserving seasonal periods of wet but not extremely dry periods in Poland (Krasiejów) and India, but a harsher climate in Morocco (Steyer et al., 2004; Konietzko-Meier & Klein, 2013; Teschner et al., 2020), favouring here the deposition of LAGs. It is similarly observed in the herein studied sample. However, the occurrence of sub-cycles and rest lines mainly in the aetosaur sample from Krasiejów, suggests that the environmental influence mostly affected the terrestrial taxon. This corresponds well with the wet and semi-dry climatic conditions as proposed in the climatic model by using analytical methods (Jewuła et al., 2019). Based on our sample, it seemed as if the environmental conditions have had more impact on the terrestrial aetosaur than on the aquatic phytosaur. Moreover, the comparative aetosaur and phytosaur samples described from localities outside Poland (USA, Argentina and Austria), show the deposition of LAGs, absent in the samples from Krasiejów, which indicates an environmental/climatic influence rather than a phylogenetic precursor.

The uninterrupted FLB deposition observed in the dinosauromorph *Silesaurus opolensis* from Krasiejów (Fostowicz-Frelik & Sulej, 2010) would either mean, that the sampled bones represent a very young individual or the silesaurid shows already a strong phylogenetic signal. All dinosaurs, even the basal ones, grew throughout most of their life with FLB (summarized in Chinsamy-Turan, 2005; Erickson, 2014). The strong phylogenetic signal in the growth of *Silesaurus* is confirmed by a similar fast uninterrupted growth in other silesaurids (i.e., *Asilisaurus kongwe* from the Middle Triassic of Tanzania, Griffin & Nesbit, 2016; *Lewisuchus admixus* from the Late Triassic of Argentina, Marsà et al., 2017; *Sacisaurus agudoensis* from Late Triassic of Brasil, Veiga et al., 2019).

Concluding, the preserved alternating pattern of zones and annuli and the absence of LAGs is observed in the poikilotherm temnospondyl amphibian (anamniote), the aetosaur and the phytosaur (amniotes) samples, co-occurring in the Krasiejów locality. This would indicate a stronger local factor influencing the growth, rather than a biological determination of growth. As this is the first study comparing various animal groups from the same locality, it can be proposed, that the external (environmental/climatic) influence was very high on the growth of poikilotherm than on endotherm animals (dinosauromorphs).

Conclusions

The growth pattern of phytosaur *Parasuchus* cf. *arenaceus* and the aetosaur *Stagonolepis olenkae*, both sampled from the locality of

Krasiejów, is very similar and a relative distinction can be made only on the level of vascularization degree (higher in aetosaurs, lower in phytosaurs) and the growth mark expression. The German phytosaur *Nicrosaurus* sp. grew in a similar pattern when compared to the Polish phytosaur *Parasuchus*. However, the *Nicrosaurus* femur shows one LAG in the outer cortex, whereas LAGS are completely absent in sectioned material from Krasiejów. Interestingly, in spite of occupying different ecological niches, bone tissue and growth pattern as well as bone compactness is rather similar in the phytosaur and aetosaur material from Krasiejów. Bone compactness analyses reveal a similar wide spectrum for the terrestrial aetosaurs (76–97%) and the semi-aquatic or aquatic phytosaurs (66–90%), questioning the reliability of compactness data alone to address the lifestyle of a taxon.

The phytosaurs as well as the aetosaur from Krasiejów differ in growth when compared to other phytosaurs (*Rutiodon*, Phytosauria indet., and *Mystriosuchus*) and aetosaurs (*Typothorax, Calyptosuchus* (= *Stagonolepis*), *Desmatosuchus, Coahomasuchus, Aetosauroides*) described from various localities. They differ by the absence of woven bone, the absent change from FLB to LZB, due to the absence of FLB deposition, the lack of LAGS, and by prolonged phases of slow growth. The latter two differences are likely related to exogenous i.e., environmental factors. From this we conclude that the climate in Krasiejów was not very seasonal with the absence of strong fluctuations but rather moderate. Our study supports the observation made before that the environmental (= adaptational) signal can override the phylogenetic signal and that the climate/environmental conditions in Krasiejów had influenced the growth pattern of at least the temnospondyl amphibians and basal archosaurs.

Acknowledgements

We are very grateful to Adam Bodzioch (University of Opole) and to Rainer Schoch (SMNS) for the access to the specimens and the permission for sectioning the material. P. Martin Sander (University of Bonn) is thanked for fruitful discussions. Olaf Dülfer (University of Bonn) is acknowledged for the preparation of the thin sections. Feiko Miedema (SMNS) is thanked for the linguistic improvement of the earlier version of the typescript. We thank the editor Alexandra Anna Enrica van der Geer and the two anonymous reviewers for the useful comments which helped to improve the quality of this paper. This work was supported by the Polish National Science Centre (NCN) grant number: UMO-2016/23/N/ST10/02179 (awarded to EMT).

References

Antczak, M. (2016). Late Triassic aetosaur (Archosauria) from Krasiejów (SW Poland): new species or an example of individual variation? *Geological Journal* 51, 779–788.

Barrett, P.M., Sciscio, L., Viglietti, P.A., Broderick, T.J., Suarez, C.A., Sharman, G.R., Jones, A.S., Munyikwa, D., Edwards, S., Chapelle, K.E.J., Dollman, K.N., Zondo, M. & Choiniere, J.N. (2020). The age of the Tashinga Formation (Karoo Supergroup) in the Mid-Zambezi Basin, Zimbabwe and the first phytosaur from mainland sub-Saharan Africa. *Gondwana Research* 81, 445–460.

Bodzioch, A. & Kowal-Linka, M. (2012). Unravelling the origin of the Late Triassic multitaxic bone accumulation at Krasiejów (S Poland) by diagenetic analysis. *Palaeogeography, Palaeoclimatology, Palaeoecology* 346, 25–36.

Brusatte, S.L., Butler, R.J., Niedźwiedzki, G., Sulej, T., Bronowicz, R. & Satkūnas, J. (2013). First record of

Mesozoic terrestrial vertebrates from Lithuania: phytosaurs (Diapsida: Archosauriformes) of probable Late Triassic age, with a review of phytosaur biogeography. *Geological Magazine* 150, 110–122.

Buffetaut E. (1993). Phytosaurs in time and space. *Pal. Lombarda. Nuov. Ser*. 2, 39–44.

Butler, R.J., Jones, A.S., Buffetaut, E., Mandl, G.W., Scheyer, T.M. & Schultz, O. (2019). Description and phylogenetic placement of a new marine species of phytosaur (Archosauriformes: Phytosauria) from the Late Triassic of Austria. *Zoological Journal of the Linnean Society* 187, 198–228.

Butler, R.J., Rauhut, O.W., Stocker, M.R. & Bronowicz, R. (2014). Redescription of the phytosaurs *Paleorhinus* (*'Francosuchus'*) *angustifrons* and *Ebrachosuchus neukami* from Germany, with implications for Late Triassic biochronology. *Zoological Journal of the Linnean Society* 170, 155–208.

Canoville, A. & Laurin, M. (2009). Microanatomical diversity of the humerus and lifestyle in lissamphibians. *Acta Zoologica* 90, 110–122.

Canoville, A. & Laurin, M. (2010). Evolution of humeral microanatomy and lifestyle in amniotes, and some comments on palaeobiological inferences. *Biological Journal of the Linnean Society* 100, 384–406.

Canoville A., de Buffrénil, V. & Laurin, M. (2016). Microanatomical diversity of amniote ribs: an exploratory quantitative study. *Biological Journal of the Linnean Society* 118, 706–733.

Carroll, R.L. (1988). *Vertebrate Paleontology and Evolution*. W.H. Freeman, San Francisco.

Cerda, I.A. & Desojo, J.B. (2011). Dermal armour histology of aetosaurs (Archosauria: Pseudosuchia), from the Upper Triassic of Argentina and Brazil. *Lethaia* 44, 417–428.

Cerda, I.A., Desojo, J.B. & Scheyer, T.M. (2018). Novel data on aetosaur (Archosauria, Pseudosuchia) osteoderm microanatomy and histology: palaeobiological implications. *Paleontology* 61, 721–745.

Chatterjee, S. (1978). A primitive parasuchid (Phytosaur) reptile from the Upper Triassic Maleri Formation of India. *Paleontology* 21, 83–127.

Chatterjee, S. (2001). *Parasuchus hislopi* Lydekker, 1885 (Reptilia, Archosauria): proposed replacement of the lectotype by a neotype. *Bulletin of Zoological Nomenclature* 58, 34–36.

Chinsamy-Turan A. (2005). *The Microstructure of Dinosaur Bone: Deciphering Biology with Fine-Scale Techniques*. Johns Hopkins University Press, Baltimore.

Cormark, D.H. (1987). *Ham's Histology*, 9th Edition. Lippincott, New York.

Cubo, J., Legendre P., de Ricqlès, A.J., Montes, L. & de Margerie, E. (2008). Phylogenetic, functional, and structural components of variation in bone growth rate of amniotes. *Evolution & Development* 10, 217–227.

Currey, J.D. (2002). *Bones: Structure and Mechanics*. Princeton University Press, Princeton, NJ.

Dasgupta, S., Ghosh, P., & Gierlowski-Kordesch, E.H. (2017). A discontinuous ephemeral stream transporting mud aggregates in a continental rift basin: the Late Triassic Maleri Formation, India. *Journal of Sedimentary Research* 87(8), 838–865.

De Buffrénil, V., de Ricqlès, A. J., Zylberberg, L., & Padian, K. (Eds.). (2021). *Vertebrate Skeletal Histology and Paleohistology*. CRC Press.

De Buffrénil, V. & Rage, J.C. (1993). La «pachyostose» vertébrale de *Simoliophis* (Reptilia, Squamata): données comparatives et considérations fonctionnelles. *Annal. Pal.*, 79, 315–335.

De Ricqlès, A.J., Padian, K. & Horner, J.R. (2003). On the bone histology of some Triassic pseudosuchian archosaurs and related taxa. *Annal. Pal.*, 89, 67–101.

De Ricqlès, A.J., Padian, K., Knoll, F. & Horner, J.R. (2008). On the origin of high growth rates in archosaurs and their ancient relatives: complementary histological studies on Triassic archosauriforms and the problem of a

"phylogenetic signal" in bone histology. *Annal. Pal.*, 94, 57–76.

Desojo, J.B., Heckert, A.B., Martz, J.W., Parker, W.G., Schoch, R.R., Small, B.J., & Sulej, T. (2013). Aetosauria: a clade of armoured pseudosuchians from the Upper Triassic continental beds. *Geological Society Special Publication* 379, 203–239.

Desojo, J.B. & Vizcaíno, S.F. (2009). Jaw biomechanics in the South American aetosaur *Neoaetosauroides engaeus*. *Paläontologische Zeitschrift* 83, 499–510.

Dróżdż, D. (2018). Osteology of a forelimb of an aetosaur *Stagonolepis olenkae* (Archosauria: Pseudosuchia: Aetosauria) from the Krasiejów locality in Poland and its probable adaptations for a scratch-digging behavior. *PeerJ*, 6, e5595.

Dzik, J. (2001). A new *Paleorhinus* fauna in the early Late Triassic of Poland. *Journal of Vertebrate Paleontology* 21, 625–627.

Dzik, J. (2003). A beaked herbivorous archosaur with dinosaur affinities from the early Late Triassic of Poland. *Journal of Vertebrate Paleontology* 23, 556–574.

Dzik, J. & Sulej, T. (2007). A review of the early Late Triassic Krasiejów biota from Silesia, Poland. *Phytopathologia Polonica* 64, 3–27.

Dzik, J. & Sulej, T. (2016). An early Late Triassic long-necked reptile with a bony pectoral shield and gracile appendages. *Acta Palaeontologica Polonica* 61, 805–823.

Dzik, J., Sulej, T., Kaim, A. & Niedźwiedzki, R. (2000). Późnotriasowe cmentarzysko kręgowców lądowych w Krasiejowie na Śląsku Opolskim. *Przegląd Geologiczny* 48, 226–235.

Erickson, G. M. (2014). On dinosaur growth. *Annual Review of Earth and Planetary Sciences* 42, 675–697.

Fostowicz-Frelik, Ł. & Sulej, T. (2010). Bone histology of *Silesaurus opolensis* Dzik, 2003 from the Late Triassic of Poland. *Lethaia* 43, 137–148.

Francillon-Vieillot, H., de Buffrénil, V., Castanet, J., Géraudie, J., Meunier, F.J., Sire, J.Y., Zylberberg, L. & de Ricqlès, A. (1990). Microstructure and mineralization of vertebrate skeletal tissues. Pp. 471–530 in: Carter, J.G. (ed), *Skeletal Biomineralization: Patterns, Processes and Evolutionary Trends*. Van Nostrand Reinhold, New York.

Gądek, K. (2012). Palaeohistology of ribs and clavicle of *Metoposaurus diagnosticus* from Krasiejów (Upper Silesia, Poland). *Opole Sci. Soc. Nat. J.* 45, 39–42.

Germain, D. & Laurin, M. (2005). Microanatomy of the radius and lifestyle in amniotes (Vertebrata, Tetrapoda). *Zool. Script.* 34, 335–350.

Górnicki, S., Antczak, M., & Bodzioch, A. (2021). Aetosaur pes from the Upper Triassic of Krasiejów (Poland), with remarks on taxonomy of isolated bones. In *Annales Societatis Geologorum Poloniae* 91, 389–396.

Gozzi, E. & Renesto, S. (2003). A complete specimen of *Mystriosuchus* (Reptilia, Phytosauria) from the Norian (Late Triassic) of Lombardy (Northern Italy). *Rivista Italiana di Paleontologia e Stratigrafi* 109, 475–498.

Griffin, C.T. & Nesbitt, S.J. (2016). The femoral ontogeny and long bone histology of the Middle Triassic (? late Anisian) dinosauriform *Asilisaurus kongwe* and implications for the growth of early dinosaurs. *Journal of Vertebrate Paleontology* 36, e1111224.

Gruntmejer, K., Konietzko-Meier, D. & Bodzioch, A. (2016). Cranial bone histology of *Metoposaurus krasiejowensis* (Amphibia, Temnospondyli) from the Late Triassic of Poland. *PeerJ*, 4, e2685.

Gruntmejer, K., Konietzko-Meier, D., Marcé-Nogué, J., Bodzioch, A. & Fortuny, J. (2019). Cranial suture biomechanics in *Metoposaurus krasiejowensis* (Temnospondyli, Stereospondyli) from the upper Triassic of Poland. *Journal of Morphology* 280, 1850–1864.

Gruntmejer, K., Bodzioch, A. & Konietzko-Meier, D. (2021). Mandible histology in *Metoposaurus krasiejowensis* (Temnospondyli, Stereospondyli) from the Upper Triassic of Poland. *PeerJ*, 9, e12218.

Hayashi, S., Houssaye, A., Nakajima, Y., Chiba, K. & Ando, T. (2012). Bone inner structure suggests increasing aquatic adaptations in *Desmostylia* (Mammalia, Afrotheria). *PLoS ONE* 8, e59146.

Heckert, A.B., Viner, T.C. & Carrano, M.T. (2021). A large, pathological skeleton of *Smilosuchus gregorii* (Archosauriformes: Phytosauria) from the Upper Triassic of Arizona, U.S.A., with discussion of the paleobiological implications of paleopathology in fossil archosauromorphs. *Palaeontologia Electronica* 24, 1–21.

Hedrick, B. P., Goldsmith, E., Rivera-Sylva, H., Fiorillo, A. R., Tumarkin-Deratzian, A. R., & Dodson, P. (2020). Filling in gaps in the ceratopsid histologic database: histology of two basal centrosaurines and an assessment of the utility of rib histology in the Ceratopsidae. *Anatomical Record* 303(4), 935–948.

Hoffman, D.K., Heckert, A.B. & Zanno, L.E. (2019). Disparate Growth Strategies within Aetosauria: Novel Histologic Data from the Aetosaur *Coahomasuchus chathamensis*. *Anatomical Record* 302, 1504–1515.

Houssaye, A. (2009) "Pachyostosis" in aquatic amniotes: a review. *Integrative Zoology* 4, 325–340.

Houssaye, A., Mazurier, A., Herrel, A., Volpato, V., Tafforeau, P., Boistel, R. & de Buffrénil, V. (2010). Vertebral microanatomy in squamates: structure, growth and ecological correlates. *Journal of Anatomy* 217, 715–727.

Houssaye, A., Rage, J.C., Bardet, N., Vincent, P., Amaghzaz, M. & Meslouh, S. (2013). New highlights about the enigmatic marine snake *Palaeophis maghrebianus* (Palaeophiidae; Palaeophiinae) from the Ypresian (Lower Eocene) phosphates of Morocco. *Palaeontology* 56, 647–661.

Houssaye, A., Sander, P. & Klein, N. (2016). Adaptive patterns in aquatic amniote bone microanatomy – more complex than previously thought. *Integrative and Comparative Biology* 56, 1349–1369.

Houssaye, A., Tafforeau, P. & Herrel, A. (2014). Amniote vertebral microanatomy – what are the major trends? *Biological Journal of the Linnean Society* 112, 735–746.

Hungerbühler, A. (2000). Heterodonty in the European phytosaur *Nicrosaurus kapffi* and its implications for the taxonomic utility and functional morphology of phytosaur dentitions. *Journal of Vertebrate Paleontology* 20, 31–48.

Hungerbühler, A. (2002). The Late Triassic phytosaur *Mystriosuchus westphali*, with a revision of the genus. *Palaeontology* 45, 377–418.

Hunt, A.P. (1989). Cranial morphology and ecology among phytosaurs. Pp. 349–354 in Lucas, S.G & Hunt, A.P. (Eds.), *Dawn of the Age of Dinosaurs in the American Southwest*. New Mexico Museum of Natural History and Science.

Hunt, A.P. & Lucas, S.G. (1991). *Rioarribasaurus*, a new name for a Late Triassic dinosaur from New Mexico (USA). *Paläontologische Zeitschrift* 65, 191.

Jewuła, K., Matysik, M., Paszkowski, M., & Szulc, J. (2019). The late Triassic development of playa, gilgai floodplain, and fluvial environments from Upper Silesia, southern Poland. *Sedimentary Geology* 379, 25–45.

Jones, A.S. & Butler, R.J. (2018). A new phylogenetic analysis of Phytosauria (Archosauria: Pseudosuchia) with the application of continuous and geometric morphometric character coding. *PeerJ*, 6, e5901.

Kammerer, C.F., Butler, R.J., Bandyopadhyay, S. & Stocker, M.R. (2016). Relationships of the Indian phytosaur *Parasuchus hislopi* Lydekker, 1885. *Papers in Palaeontology* 2, 1–23.

Kawano, S.M., Economy, D.R., Kennedy, M.S., Dean, D., & Blob, R.W. (2016). Comparative limb bone loading in the humerus and femur of the tiger salamander: testing the 'mixed-chain' hypothesis for skeletal safety factors. *Journal of Experimental Zoology* 219, 341–353.

Kimmig, J. (2013). Possible secondarily terrestrial lifestyle in the European phytosaur *Nicrosaurus*

kapffi (Late Triassic, Norian): a preliminary study. *Bulletin - New Mexico Museum of Natural History and Science* 61, 306–312.

Klein, N., & Sander, P.M. (2007). Bone histology and growth of the prosauropod dinosaur *Plateosaurus engelhardti* (von Meyer 1837) from the Norian bonebeds of Trossingen (Germany) and Frick (Switzerland). *Spec. Pap. Pal.* 77, 169–206.

Klein, N., Sander, M. & Suteethorn, V. (2009). Bone histology and its implications for the life history and growth of the Early Cretaceous titanosaur *Phuwiangosaurus sirindhornae*. *Geological Society Sspecial Publication* 315, 217–228.

Klein, N., Foth, C. & Schoch, R.R. (2017). Preliminary observations on the bone histology of the Middle Triassic pseudosuchian archosaur *Batrachotomus kupferzellensis* reveal fast growth with laminar fibrolamellar bone tissue. *Journal of Vertebrate Paleontology* 37, e1333121.

Klein, N., Houssaye, A., Neenan, J. M. & Scheyer, T. M. (2015). Long bone histology and microanatomy of Placodontia (Diapsida: Sauropterygia). *Contributions to Zoology* 84, 59–84.

Köhler, M., Marín-Moratalla, N., Jordana, X., & Aanes, R. (2012). Seasonal bone growth and physiology in endotherms shed light on dinosaur physiology. *Nature* 487(7407), 358–361.

Konietzko-Meier, D. & Klein, N. (2013). Unique growth pattern of *Metoposaurus diagnosticus krasiejowensis* (Amphibia, Temnospondyli) from the Upper Triassic of Krasiejów, Poland. *Palaeogeography, Palaeoclimatology, Palaeoecology* 370, 145–157.

Konietzko-Meier, D. & Sander, P.M. (2013). Long bone histology of *Metoposaurus diagnosticus krasiejowensis* (Temnospondyli) from the Late Triassic of Krasiejów (Opole, Silesia Region). *Journal of Vertebrate Paleontology* 33, 1003–1018.

Konietzko-Meier, D., Bodzioch, A. & Sander, P.M. (2012). Histological characteristics of the vertebral intercentra of *Metoposaurus diagnosticus* (Temnospondyli) from the Upper Triassic of Krasiejów (Upper Silesia, Poland). *Earth and Environmental Science Transactions of the Royal Society of Edinburgh* 103, 237–250.

Konietzko-Meier, D., Danto, M. & Gądek, K. (2014). The microstructural variability of the intercentra among temnospondyl amphibians. *Biological Journal of The Linnean Society* 112, 747–764.

Konietzko-Meier, D., Gruntmejer, K., Marcé-Nogué, J., Bodzioch, A. & Fortuny, J. (2018). Merging cranial histology and 3D-computational biomechanics: a review of the feeding ecology of a Late Triassic temnospondyl amphibian. *PeerJ* 6, e4426.

Kriloff, A., Germain, D., Canoville, A., Vincent, P. & Sache, M. (2008). Evolution of bone microanatomy of the tetrapod tibia and its use in palaeobiological inference. *Journal of Evolutionary Biology* 21, 807–826.

Laurin, M., Canoville, A. & Germain, D. (2011). Bone microanatomy and lifestyle: a descriptive approach. *Comptes Rendus Palevol* 10, 381–402.

Lees, J.H. (1907). The skull of *Paleorhinus*: a Wyoming phytosaur. *Journal of Geology* 15, 121–151.

Li, C., Wu, X.C., Zhao, L.J., Sato, T. & Wang, L.T. (2012). A new archosaur (Diapsida, Archosauriformes) from the marine Triassic of China. *Journal of Vertebrate Paleontology* 32, 1064–1081.

Lucas, S.G. (1998). Global Triassic tetrapod biostratigraphy and biochronology. *Palaeogeography, Palaeoclimatology, Palaeoecology* 143, 347–384.

Marsà, J.A.G., Agnolín, F.L. & Novas, F. (2017). Bone microstructure of *Lewisuchus admixtus* Romer, 1972 (Archosauria, Dinosauriformes). *Historical Biology* 31, 157–162.

Marsh, O.C. (1884). The classification and affinities of dinosaurian reptiles. *Nature* 31, 68–69.

Mateus, O., Butler, R. J., Brusatte, S. L., Whiteside, J. H. & Steyer, J.-S. (2014). The first phytosaur (Diapsida, Archosauriformes) from the Late Triassic of the Iberian Peninsula. *Journal of Vertebrate Paleontology* 34, 970–975.

Nesbitt, S.J. (2011). The early evolution of archosaurs: relationships and the origin of major clades. *Bulletin of the American Museum of Natural History* 352, 1–292.

Nitsch, E. (2006). Der Keuper. Zeitreise ins Dinosaurierland. *Biologie in unserer Zeit* 36, 374–383.

Parker, W.G., Stocker, M.R. & Irmis, R.B. (2008). A new desmatosuchine aetosaur (Archosauria: Suchia) from the Upper Triassic Tecovas Formation (Dockum Group) of Texas. *Journal of Vertebrate Paleontology* 28, 692–701.

Pereyra, M.E., Bona, P., Cerda, I.A., Jannello, J.M., De La Fuente, M.S. & Desántolo, B. (2020). Growth dynamics and body size evolution of South American long-necked chelid turtles: A bone histology approach. *Acta Palaeontologica Polonica* 65, 535–545.

Ponce, D. A., Desojo, J. B. & Cerda, I. A. (2022). Palaeobiological inferences of the aetosaur *Aetosauroides scagliai* (Archosauria: Pseudosuchia) based on microstructural analyses of its appendicular bones. *Historical Biology*. doi:10.1080/08912963.2022.2035728.

Renesto, S. (2008). Remains of a juvenile phytosaur from the Late Triassic of northern Italy. *Rivista Italiana di Paleontologia e Stratigrafia* 114, 155–160.

Renesto, S. & Paganoni, A. (1998). A phytosaur skull from the Norian (Late Triassic) of Lombardy (northern Italy). *Rivista Italiana di Paleontologia e Stratigrafia* 104, 115–122.

Roberto-Da-Silva, L., Desojo, J.B., Cabreira, S.F., Aires, A.S., Mueller, R.T., Pacheco, C.P. & Dias-Da-Silva, S. (2014). A new aetosaur from the Upper Triassic of the Santa Maria Formation, southern Brazil. *Zootaxa*, 3764, 240–278.

Scheyer, T.M., Desojo, J.B. & Cerda, I.A. (2014). Bone histology of phytosaur, aetosaur, and other archosauriform osteoderms (Eureptilia, Archosauromorpha). *Anatomical Record* 297, 240–260.

Seitz, A.L.L. (1907). Vergleichende Studien über den mikroskopischen Knochenbau fossiler und rezenter Reptilien und dessen Bedeutung für das Wachstum und Umbildung des Knochengewebes im allgemein. *Nova Acta Leop. Abh. Deu. Aka. Naturforsch.*, 37, 230–370.

Small, B.J. (2002). Cranial anatomy of *Desmatosuchus haplocerus* (Reptilia: Archosauria: Aetosauria). *Zoological Journal of the Linnean Society* 136, 97–111.

Steyer, J.S., Laurin, M., Castanet, J. & de Ricqlès, A. (2004). First histological and skeletochronological data on temnospondyl growth: palaeoecological and palaeoclimatological implications. *Palaeogeography, Palaeoclimatology, Palaeoecology* 206, 193–201.

Stocker, M.R. & Butler, R.J. (2013). Phytosauria. In: Nesbitt, S.J., Desojo, J.B.& Irmis, R.B. (Eds.), Anatomy, Phylogeny and Palaeobiology of Early Archosaurs and Their Kin. *Geological Society Special Publications* 379, 91–117.

Stocker, M.R., Zhao, L.J., Nesbitt, S.J., Wu, X.C. & Li, C. (2017). A short-snouted, Middle Triassic phytosaur and its implications for the morphological evolution and biogeography of Phytosauria. *Scientific Reports* 7, 1–9.

Sulej, T. (2005). A new rauisuchian reptile (Diapsida: Archosauria) from the Late Triassic of Poland. *Journal of Vertebrate Paleontology* 25, 78–86.

Sulej, T. (2007). Osteology, variability, and evolution of *Metoposaurus*, a temnospondyl from the Late Triassic of Poland. *Pal. Pol.*, 64, 29–139.

Sulej, T. (2010). The skull of an early Late Triassic aetosaur and the evolution of the stagonolepidid archosaurian reptiles. *Zoological journal of the Linnean Society* 158, 860–881.

Sulej, T., & Majer, D. (2005). The temnospondyl amphibian *Cyclotosaurus* from the Upper Triassic of Poland. *Palaeontology*, 48, 157–170.

Szulc, J. (2005). Sedimentary environments of the vertebrate-bearing Norian deposits from Krasiejów, Upper Silesia (Poland). *Hallesches Jahrbuch für Geowissenschaften* 19, 161–170.

Szulc, J. & Racki, G. (2015). Formacja grabowska: podstawowa jednostka litostratygraficzna kajpru Górnego Śląska. *Przegląd Geologiczny* 63, 103–113.

Szulc, J., Racki, G., Jewuła, K. & Środoń, J. (2015). How many Upper Triassic bone–bearing levels are there in Upper Silesia (southern Poland)? A critical overview of stratigraphy and facies. *Annales Societatis Geologorum Poloniae* 85, 587–626.

Szulc, J., Racki, G. & Bodzioch, A. (2017). Comment on "An early Late Triassic long-necked reptile with a bony pectoral shield and gracile appendages" by Jerzy Dzik and Tomasz Sulej. *Acta Palaeontologica Polonica* 62, 287–288.

Teschner, E.M., Sander, P.M. & Konietzko-Meier, D. (2018). Variability of growth pattern observed in *Metoposaurus krasiejowensis* humeri and its biological meaning. *Journal of Iberian Geology* 44, 99–111.

Teschner, E.M., Chakravorti, S., Sengupta, D.P. & Konietzko-Meier, D. (2020). Climatic influence on the growth pattern of *Panthasaurus maleriensis* from the Late Triassic of India deduced from paleohistology. *PeerJ* 8, e9868.

Veiga, F.H., Botha-Brink, J., Ribeiro, A., Ferigolo, J. & Soares, M.B. (2019). Osteohistology of the silesaurid *Sacisaurus agudoensis* from southern Brazil (Late Triassic) and implications for growth in early dinosaurs. *Anais. Acad. Brasil. Ciênc.*, 91, 1–17 e20180643.

Von Jäger, G.F. (1828). *Über die fossilen Reptilien, welche in Württemberg aufgefunden worden sind*. Stuttgart: Metzler.

Von Meyer, H. (1861). Reptilien aus dem Stubensandstein des oberen Keupers. *Palaeontographica* 7, 253–346.

Walker, A. D. (1961). Triassic reptiles from the Elgin area: *Stagonolepis, Dasygnathus* and their allies. *Philosophical transactions of the Royal Society of London. Series B, Biological Sciences* 244, 103–204.

Witzmann, F., Schoch, R.R., Hilger, A. & Kardjilov, N. (2012). Braincase, palatoquadrate and ear region of the plagiosaurid *Gerrothorax pulcherrimus* from the Middle Triassic of Germany. *Palaeontology*, 55, 31–50.

Woodward, H.N., Horner, J.R. & Farlow, J.O. (2014). Quantification of intraskeletal histovariability in *Alligator mississippiensis* and implications for vertebrate osteohistology. *PeerJ*, 2, e422.